Integrated Economic Dispatch and Demand Response Model for Grid-Game Simulation that Incorporates Electric Vehicle Charging Loads and Renewable Generation

A Thesis

Presented in Partial Fulfillment of the Requirements for the

Degree of Master of Science

with a

Major in Electrical Engineering

in the

College of Graduate Studies

University of Idaho

by

Nathan G. Davis

Major Professor: Brian K. Johnson, Ph.D.

Committee Members: Herbert L. Hess, Ph.D.; Yacine Chakhchoukh, Ph.D.

Department Administrator: Mohsen Guizani, Ph.D.

December 2016

Authorization to Submit Thesis

This thesis of Nathan G. Davis, submitted for the degree of Master of Science with a major in Electrical Engineering and titled "Integrated Economic Dispatch and Demand Response Model for Grid-Game Simulation that Incorporates Electric Vehicle Charging Loads and Renewable Generation," has been reviewed in final form. Permission, as indicated by the signatures and dates given below, is now granted to submit final copies to the College of Graduate Studies for approval.

Major Professor: _____Date_____
Brian K. Johnson, Ph.D.

Committee Members: _____Date_____
Herbert L. Hess, Ph.D.

_____Date_____
Yacine Chakhchoukh, Ph.D.

Department Administrator: _____Date_____
Mohsen Guizani, Ph.D.

Abstract

In this thesis, a unit commitment model is developed that integrates economic dispatch and demand response into a single mixed integer linear program which is formulated to include renewable generation and electric vehicle charging. The objective function is expressed as a cost function formulated to minimize cost of generation and to penalize curtailment of load. The constraints ensure that energy balance, ramp rate limits, and transmission limits are observed. To support the integrated model, separate generation and load models are developed from historical data collected from Department of Energy research laboratories and from stochastic approximations. Renewable generation is integrated into the generation model as non-curtailable sources to demonstrate the variability introduced into the system and to stress the model. In addition, electric vehicle charging systems are included in the load model to determine the impact that various levels of electric vehicle penetration has on residential and commercial loads. The model is then used to simulate a hypothetical grid connected microgrid that can import power from external sources. An interactive user interface allows the user to modify the system to observe the response with the objective of maximizing profit. The thesis concludes by presenting a novel approach to the solution of difference equations using mixed integer linear programs that have been developed in this project and that can be further developed and extended to provide an alternative to z-transform analysis or iterative numerical methods.

Acknowledgements

I would like to thank Tim McJunkin who provided me the opportunity to develop these concepts while working with him at Idaho National Laboratories during the Summer of 2016. Without his efforts to secure funding from the EV Everywhere initiative and through the Office of Energy Efficiency and Renewable Energy, I would not have had the success I did in developing the project.

I would also like to thank Dr. Brian Johnson and Dr. Herbert Hess for their exceptional instruction and guidance in and out of the classroom. Both reflect the commitment and integrity that I hope to emulate in all endeavors that I pursue in the future.

In addition, I would like to thank the unnamed contributors to Wikipedia who developed the LaTeX WikiBook. Without this invaluable resource, it is unlikely that this Thesis would have been produced.

Finally, I would like to thank my wife, Jonna, who has encouraged me and patiently allowed me to pursue this endeavor. She has been the willing reviewer and insightful critic when I have needed it most and has unconditionally encouraged me through all stages of this effort.

Dedication

To my Mom,

who provided me a great childhood that fostered my curiosity and love of learning.

If I could, I would not change a thing.

Table of Contents

List of Tables

List of Figures

List of Equations

Glossary

$a_{i,j}$	...	i^{th} coefficient of the j^{th} constraint for the standard linear programming problem
b_j	...	j^{th} constraint constant for the standard linear programming problem
c_n	...	n^{th} cost coefficient for standard linear programming problem
C_i	...	i^{th} cost coefficient for the integrated dispatch algorithm
$C_f(i)$	...	i^{th} fuel cost coefficient for a generation element
$C_{op}(i,t)$	...	i^{th} operating cost coefficient for a generation element
$F(i,t)$	...	Fuel function for the i^{th} generation element
$G_{RH}(n\Delta t)$	...	Run of the river hydro-electric generation for timestep n
$G_{RS}(n\Delta t)$	...	Solar generation for timestep n
$G_{RW}(n\Delta t)$	...	Wind generation for timestep n
$G_{SM}(n\Delta t)$	...	Power from spot market purchase for timestep n
H_s	...	Historical normal incident solar radiation (W/m^2)
$I(i,t)$	...	i^{th} decision variable for t^{th} timestep for the integrated dispatch algorithm
$L_{R,C,I}(n\Delta t)$	...	Total load at the n^{th} timestep of type (R)esidential, (C)ommercial, and (I)ndustrial from historical data
N_G	...	Total number of generation elements
N_L	...	Total number of load elements
N_{RH}	...	Total number of renewable hydro-electric elements
$N_{R,C,I}$	...	Total number of (R)esidential, (C)ommercial, and (I)ndustrial load elements
N_S	...	Total number of solar generation elements
N_{SM}	...	Total number of spot market contracts
N_W	...	Total number of wind generation elements

P_{min}	...	Minimum power threshold
P_{max}	...	Maximum power threshold
P_{RH}	...	Peak generation capacity of renewable hydro-electric element
P_S	...	Peak generation capacity of solar array
P_{SM}	...	Peak power available from spot markets
P_W	...	Peak generation capacity of wind resource
$P(i,t)$	...	Power rating for the i^{th} element at the t^{th} timestep for the integrated dispatch algorithm
$P_G(i,t)$	...	Power rating for the i^{th} generator element at the t^{th} timestep for the integrated dispatch algorithm
$P_L(i,t)$	...	Power rating for the i^{th} load element at the t^{th} timestep for the integrated dispatch algorithm
$Q_{RH}(n\Delta t)$	...	Historical volumetric flowrate (m^3/hr)
$\rho_c(i)$	...	penalty cost associated with the i^{th} load element
$r_s(i,t)$	...	Spinning reserve of i^{th} generation element
$R_s(t)$	...	Total spinning reserve in system
$R_u(i)$	...	Ramp up limit of the i^{th} generation element
$R_d(i)$	...	Ramp down limit of the i^{th} generation element
ΔST	...	Change in the state of charge of storage element
ST_{sink}	...	Storage sink element
ST_{source}	...	Storage source element
$Y_{R,C,I}(n\Delta t)$	...	Historical data at the n^{th} timestep of type (R)esidential, (C)ommercial, and (I)ndustrial
ν_w	...	Historical wind speed data (m/s)
x_n	...	n^{th} decision variable for standard linear programming problem for the integrated dispatch algorithm

Chapter 1: Introduction

Renewable energy resources coupled with the introduction of electric vehicle technology has the potential to significantly reduce dependence on carbon emitting generation from coal and gas fired power plants and thereby help to reduce green house gas emissions. Current policy recognizes this and has introduced incentives to encourage investment in both renewable generation and electric vehicle technologies. As a result, estimates from 2010 show that approximately 11.6% of the total electrical energy capacity of the United States was from renewable generation [1], which is expected to represent 70% of all new generation capacity added between now and 2030 [2]. In addition, it was estimated in 2012 that there were approximately 40,000 electric vehicles sold in the United States [3] and sales were expected to grow by 12.2% annually until 2035.

The driving factors behind these technologies however are not the incentives. Investment in renewable generation and electric vehicle technology represent sound investments that can generate significant profits and lower the cost of generation or operation. As an example, a study by Deloitte Touche Tohmatsu Limited, an audit and financial services consultant, reported that wind turbines generally require four to six years to provide a return on investment and the probability of generating an internal rate of return exceeding 9% was 86% [4]. Given the expected service life is approximately 25 years, investments in wind generation facilities represent a 20 year revenue stream that is only impacted by maintenance and operational expenses. In the case of electric vehicles, it is estimated that for the current state of technology, the equivalent fuel cost would be $0.70 per gallon and that two out of every three gallons of gasoline could be eliminated if the vehicle had an operating range of only 40 miles [7]. However, while these technologies provide sound investment opportunities and greatly benefit the environment, they are not without challenges. In the next two sections, a brief introduction to electric vehicles and renewable generation is presented along with a summary of some of the challenges that these technologies present.

1.1 Electric Vehicle Technology and Charging Systems

Early development of electric vehicles resulted from the introduction of the dynamo and the lead acid battery in the mid 19^{th} century. Steam technology during that period went through a significant growth phase and, as a result, the potential of early electric vehicles was unrealized and only occupied a niche market. At the beginning of the 20^{th} century, several competing technologies including hydrogen powered vehicles, electric vehicles, and the internal combustion engine were vying for market share. Ultimately, the introduction of the assembly line by Henry Ford to produce the first generation of vehicles powered by the internal combustion engine trumped the other technologies and led the electric vehicle to near extinction until the 1980's. Figure 1.1 shows the significant events that influenced electric vehicles since the Faraday first demonstrated the electro-magnetic phenomena in 1821 to the introduction of the first hybrid electric vehicle by General Electric in 1982.

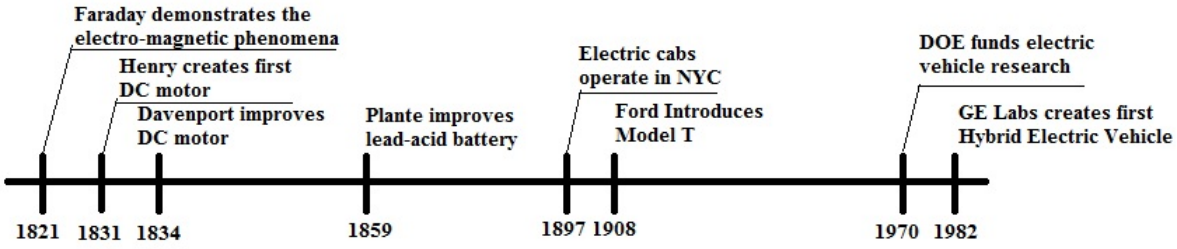

Figure 1.1: Projected Hybrid and Electric Vehicle Sales [5]

Today, electric vehicle technology has developed along several different pathways. As outlined in [7], these pathways have led to two distinct types of electric vehicles. The first to develop were the pure electric vehicles which evolved from the early research. These vehicles are characterized as only possessing an electric motor and on-board battery storage available for locomotion and that can be recharged by either using a plug-in connector or by replacing the depleted battery packs. Vehicles of this type that are recharged using a connector are commonly referred to as plug-in electric vehicles (PEV) and are experiencing a significant

amount of investment and research. While these vehicles have high efficiency ratings, they tend to have a limited range as opposed to vehicles with internal combustion engines due to the lower energy density of the batteries. This limitation is becoming less of an issue as battery technology and vehicle efficiency improves but still limits market share when coupled with the additional expense introduced by the battery packs.

The second type of electric vehicle to emerge is referred to as a hybrid-electric vehicle. This type of electric vehicle uses both an internal combustion engine and an electric motor for locomotion. These vehicles have different configurations and are referred to as either *parallel* or *series* hybrids. In the case of the parallel hybrid, both the internal combustion engine and electric motor are mechanically coupled to the transmission and can be used in conjunction with each other to improve fuel efficiency. In the latter case, the series hybrids, which are sometimes referred to as *extended range electric vehicles*, mechanically couple the electric motors to the drive system and use the internal combustion engine for on-board charging of the batteries. Both types of hybrids improve mileage, however they still produce tailpipe emissions. In addition, since both an internal combustion engine and electrical system are present, these type of vehicles are technically more complex than pure electric vehicles. They do benefit however from a lower initial cost as a result of lower reliance on battery storage.

As mentioned earlier, sales of electric vehicles are expected to grow by approximately 12% per year until the mid-2030's. As seen in Figure 1.2, hybrid vehicles are expected to outpace pure electric vehicles with an expected annual sales in excess of 100,000 units per year by 2030. As electric vehicles become more common, charging systems are being developed to provide various types of charging options for the consumer. As shown in Table 1.1, there are four primary modes defined for electric vehicle charging systems [7]. The first two modes are representative of residential based charging systems and can result in electrical loads of up to $10kW$ with charge times between four and eight hours. While this will increase the total load on the grid, slow charging will likely occur in the evening hours during periods of low demand and therefore limit the need for significant investment in additional infrastructure.

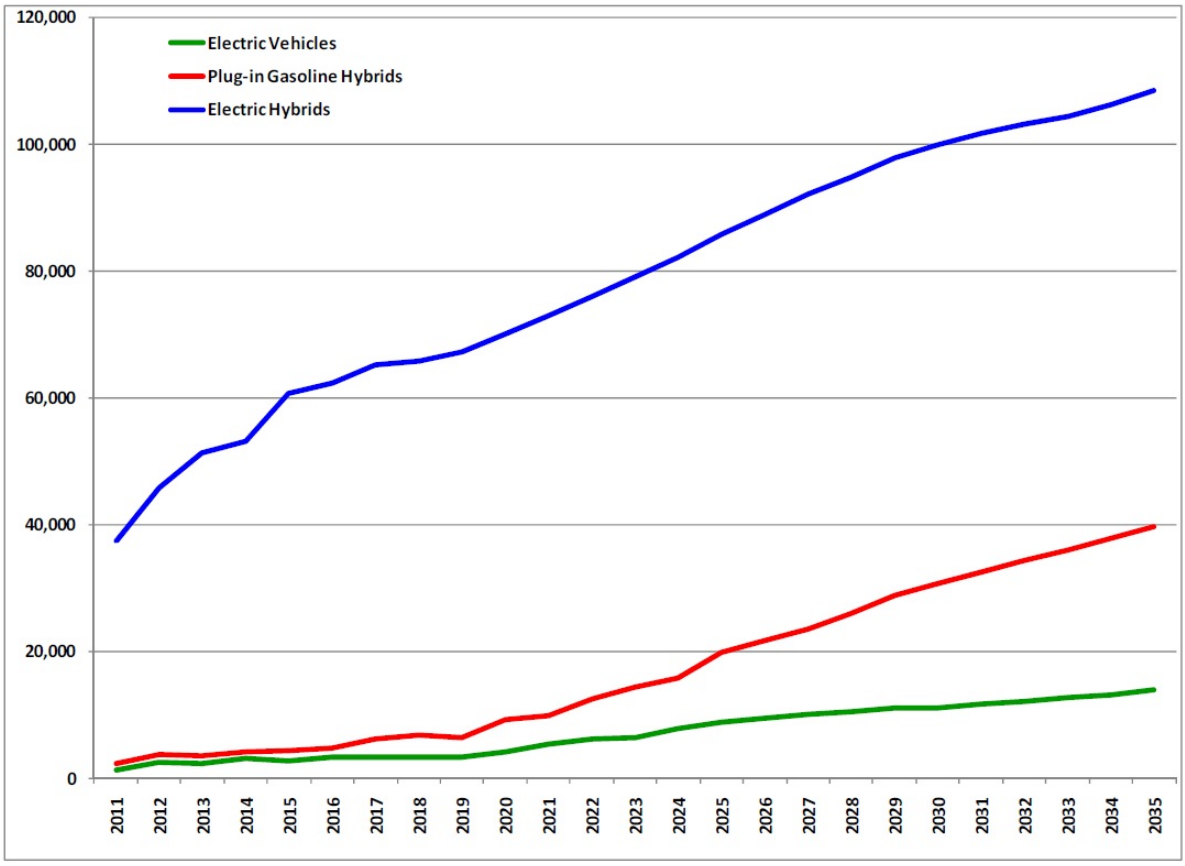

Figure 1.2: Projected Hybrid and Electric Vehicle Sales [3]

Further, the advent of smart charging systems will allow utilities to control charge periods and supplement existing demand response strategies, which provides load leveling capability by curtailment of electric vehicle charging which will be beneficial to grid operations.

Table 1.1: Electric Vehicle Charging System Characteristics

Type	$V_{nominal}$	$I_{nominal}$	$P_{nominal}$	Charge Time	Application
1	120 V	15 A	1.4 kW	18 hours	Residential
2	220 V	15 A	3.3 kW	8 hours	Residential
3	220 V	30 A	6.6 kW	4 hours	Residential/Commercial
4	480 V	167 A	50-70 kW	20-50 minutes	Commercial

The latter two modes of electric vehicle charging systems are targeted for commercial installations with electrical loads ranging from 22 kW to 120 kW depending on the type of charging system deployed. These systems will reduce charge times to between 10 minutes and two hours depending on the type of system used, but will represent a significant short term

load on the distribution network. In particular, since it is anticipated that these charging systems will be highly utilized during the afternoon hours for the return commute, this new load will occur during peak load hours and will introduce significant stress on the distribution system. This can be offset by dynamic scheduling of charging, but will require development of infrastructure before a strategy such as this is realized.

1.2 Renewable Energy Resources and Challenges

Many technologies have been developed to harness power from renewable resources. Various cultures have used hydro power for centuries to grind grain into flour while others used wind to fill the sails that allowed early exploration and establishment of trade routes. It is only natural then that hydro-electric generation was among the earliest form of renewable generation to be developed for electrical power production. The modern hydro-electric turbine was developed from the water turbine introduced by Bernard Forest de Bélidor in the mid 18th century [6]. A little more than a century later, this technology was coupled with the recently developed dynamo in the late 1880's to power the electric street lamps in Michigan and New York. Since that time, advances in material science and civil engineering have allowed earthen dams to be replaced with concrete dams that not only create the hydraulic head required to generate electricity, but also provide flood control in the river valleys and navigable waterways for commerce.

Today, new development of hydro-electric generation facilities is limited due to regulatory constraints and limited availability of hydro-geological resources. Because of this, the renewable energy supply from hydro-electric facilities has remained relatively constant for the past ten years as seen in Figure 1.3. Fortunately, hydro-electricity is but one of a multitude of renewable energy resources that are used to meet the electrical demand. Other resources include wind, solar, geothermal, and a variety of biomass fuels with each presenting opportunities and challenges. As an example, current trends show that the majority of investment in renewable generation is in the form of wind turbine facilities with forecasts

expecting generation from wind to reach 6% of the United States total energy capacity by the end of 2017 [8]. This is partially driven by the short term return on investment and the long service life that wind generation facilities provide. Unfortunately, wind is currently among the most difficult renewable resource to utilize because of high variability. Generally, site selection is based on extended average wind speed studies that attempt to assess the viability of the wind resources in region. Since wind speed can vary rapidly, short term variability can significantly limit the amount of power that a wind turbine can produce or that the electrical grid can use. As with other renewable energy technologies, this will become less of a challenge as large scale grid storage becomes available.

As seen in Figure 1.3, the overall renewable energy supply available is increasing by approximately 5% per year with significant growth in both solar and wind capacity. This trend is expected to continue as the United States and other countries move away from technologies that generate greenhouse gasses and adopt environmentally friendly renewable generation.

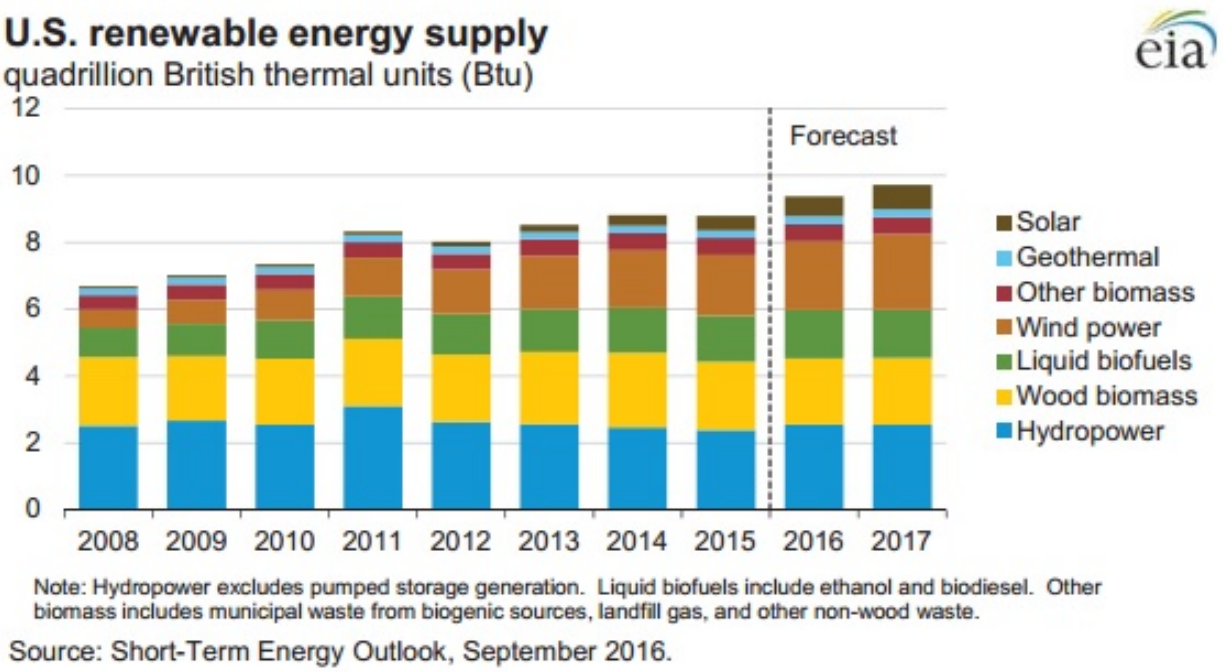

Figure 1.3: Annual Renewable Energy Supply [8]

1.3 Objectives and Path Forward

Because of the rapid increase in the penetration of renewable generation and electric vehicle charging systems, efforts are underway to develop models that can adequately commit and dispatch resources to satisfy consumer demand while adequately modeling the physics of the system. Most research is currently focused on considering renewable generation and electric vehicle charging systems in isolation from the context of either the economic dispatch or the unit commitment problem. Therefore, there exists a need to identify a method that allows for the inclusion of generation from renewable resources and load from electric vehicle charging systems. This paper will propose such a method by satisfying the following objectives.

1. Select an appropriate level of control that allows for inclusion of traditional generation and storage, renewable energy resources, and electric vehicle charging systems.
2. Identify data sources of sufficient fidelity to accurately model renewable generation resources.
3. Identify data sources and models of sufficient fidelity to accurately model residential, commercial, and industrial loads.
4. Implement the control algorithm iteratively so that system behavior can be considered for extended periods.

To satisfy these objectives, this work is organized as follows. Chapter 2 provides a brief introduction to linear programming followed by a description of the unit commitment, economic dispatch and demand response problems. It concludes with a discussion of the mixed integer linear program developed for their integration. Chapter 3 provides an in-depth description of the generation and load models used as inputs to the integrated dispatch model. Chapter 4 continues by describing the simulation developed to test the linear programming model. The results, which were published in the fourth annual IEEE Technologies for Sustainability Conference, are presented in Chapter 5. Finally, Chapter 6 presents and discusses

the conclusions drawn from this research and highlights opportunities for future works that could be developed from it.

Chapter 2: Development of the Integrated Dispatch Algorithm

In their infancy, power systems developed from localized distribution systems connecting one or more load centers to centralized generation. As population centers expanded and demand increased, technological advances allowed the migration to large bulk generation sources such as coal fired generation which were required to provide a more economically viable means of power production. As a result, transmission systems were developed to interconnect the generation resources to increase reliability and reduce costs. This approach lead to the formation of complex, non-linear systems which were difficult to analyze and introduced stability and reliability issues as well as environment concerns.

To address these issues, current trends are moving away from bulk generation and instead are utilizing distributed generation to satisfy all or part of local demand. If these distributed generation resources are locally controlled, they can allow a distribution network to operate independent of the larger power system. These systems are often referred to as microgrids and can include distributed generation in the form of diesel or gas-fired generators, photovoltaic arrays, wind turbines, or a variety of other technologies that are still in early stages of development. As mentioned previously, grid level storage tends to be impractical, however storage becomes more feasible in a microgrid configuration due to the smaller scale. But what is a microgrid? In 2012, CIGRÉ study committee C6 defined a microgrid as:

> "a group of interconnected loads and distributed energy resources within clearly defined electrical boundaries that acts as a single controllable entity with respect to the grid. A microgrid can connect and disconnect from the grid to enable it to operate in both grid-connected or island-mode." [13]

As is evidenced by this definition, microgrids can provide better reliability and power quality because of their ability to operate independent of the larger system. In addition, they can reduce peak power requirements by locally controlling unit commitment and dispatch in response to changes in demand [12]. However, in order to achieve this, microgrid control systems need to adequately control the system during both grid connected and is-

landed modes of operation. As a result, these control systems have been developed to utilize a hierarchical topology composed of four levels [10]. Each level has different tasks and responsibilities assigned to it and must coordinate with the other levels to allow the system to operate either independently or in grid connected mode. Further, the control system must maintain synchronism with the external grid to allow the system to reconnect to the grid after operating in island-mode.

At the lowest level of the microgrid control system hierarchy is the primary level which provides primary frequency control for the system through the use of a droop frequency controller. The droop controller responds to input from the secondary level which uses a proportional-integral (PI) controller to respond to changes in bus voltage magnitudes and phase angles in the system. These voltages are assigned at the tertiary level to achieve the desired active and reactive power flow between the buses. Finally, at the quaternary level, the active and reactive power flows themselves are determined from the economic dispatch and unit commitment problems in order to satisfy energy conservation and other system constraints. The low level control of the system at the primary and secondary levels requires real time response to maintain system stability. At the higher levels, the control system predicts power requirements across multiple prediction horizons to allow for 15 minute ahead, hour ahead, and even day ahead forecasting of demand. This allows the system to commit thermal and other generation units in advance of demand to ensure availability of the generation resources.

Earlier investigations and simulations of microgrids developed for a course offered by Idaho National Lab led to a gamefication referred to as the "GridGame"[11]. This simulation was developed to represent the behavior of a microgrid control system from the point of view of the secondary level of this hierarchy and used a finite difference approximation of a PI controller to maintain frequency stability in the system. In order to allow for the gamification of the simulation, a pricing structure was assigned to the energy generation along with limited control capability for the player, who acted as an independent system

operator (ISO). This implementation provided high fidelity as a result of the short timestep required by the swing equation but limited the size of the data sets that could be analyzed. In addition, this implementation included only a limited number of generation types and did not include support for electric vehicle charging systems. As a result, a conceptual model was developed at a longer time scale that could integrate a variety of generation and load types. This conceptual model, developed by Tim McJunkin at Idaho National Laboratory, is represented by the block diagram shown in Figure 2.1.

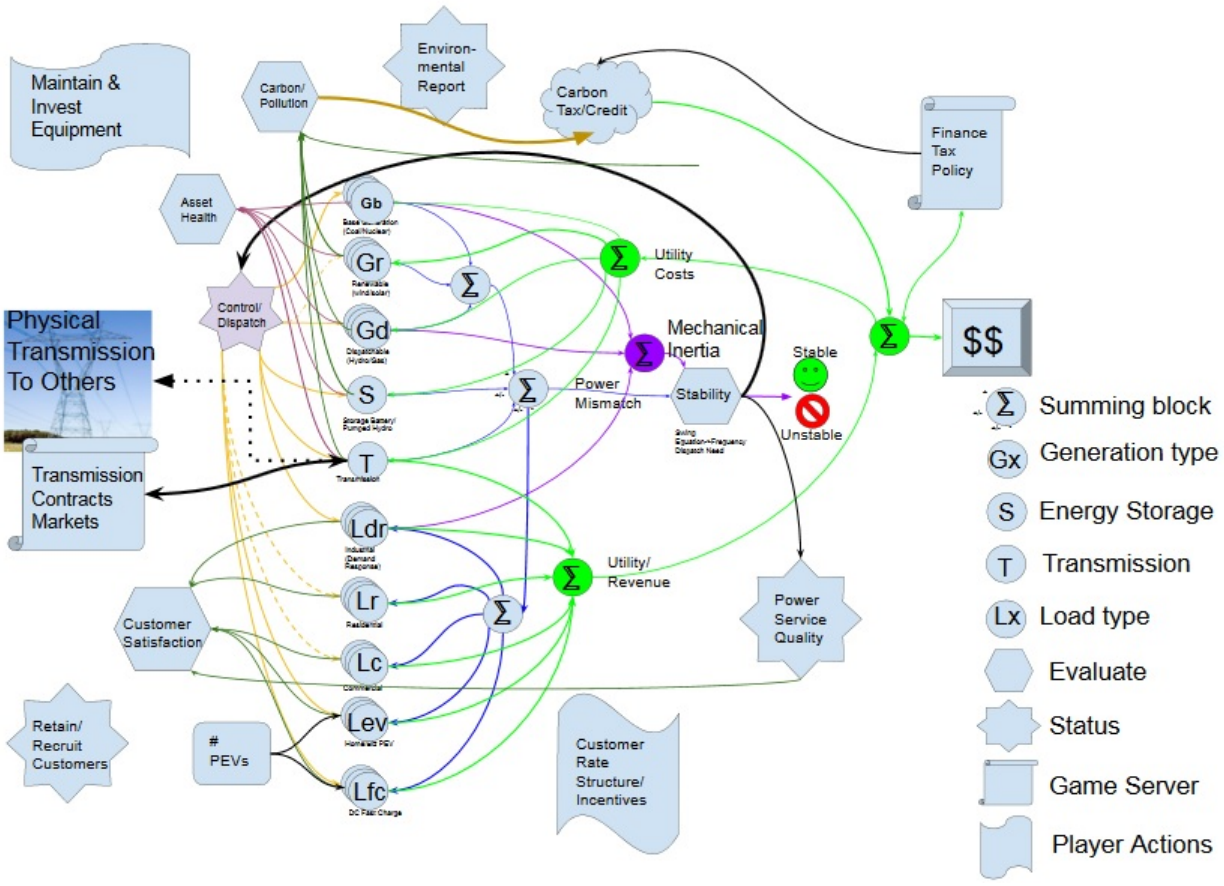

Figure 2.1: Medium Time Scale Block Diagram

The simulation described in Chapters 3 and 4 use the GridGame and this block diagram as its basis. It implements the microgrid control at the tertiary level where the economic dispatch, demand response, and unit commitment problems determine the combination of generation units and levels of production required to meet demand. This allows the simu-

lation to be implemented over extended periods and can be used with multi-year data-sets to analyze long term behavior of the system. These problems, as described above, make predictions based on current and historical demand. Before proceeding to the formulation of the resulting integrated approach developed in this research, a brief review of linear programming will be provided followed by a summary of each of these problems in the following sections.

2.1 Summative Review of Linear Programming

Linear programming refers to an optimization technique used to determine the optimal value that an objective function can achieve when subject to one or more constraints [16]. It distinguishes itself from other optimization techniques in that both the objective function and the constraints are modeled as linear relations constructed as linear combinations of decision variables (x_i) and constant coefficients c_i. Because of this, each decision variable is required to be linearly independent. In some circumstances, it is desirable to *couple* two or more decision variables such that an action on one influences the outcome of the other. To maintain independence of the decision variables, a coupling constraint can be used to restrict the behavior of the coupled variables.

The standard form of a linear programming problem, as seen in Eq. (2.1), defines the objective to maximize the function, but can be defined to minimize functions as well [16]. The constraints define the feasibility region for the system as a convex polytope and are here represented as a system of inequalities. As will be seen, these are more commonly expressed singularly to allow for descriptors to be included in the linear programming model. In addition, while it is common to express the constraints as strict inequalities, each constraint

can represent either an inequality defined on an open or closed interval or as an equality.

Objective Function:

$$maximize \sum_{n=1}^{N} (c_n x_n)$$

Subject to:

$$\begin{bmatrix} a_{11} & a_{12} & \dots & a_{1n} \\ a_{21} & a_{22} & \dots & a_{2n} \\ \vdots & \vdots & \ddots & \vdots \\ a_{m1} & a_{m2} & \dots & a_{mn} \end{bmatrix} \begin{bmatrix} x_1 \\ x_2 \\ \vdots \\ x_n \end{bmatrix} \leq \begin{bmatrix} b_1 \\ b_2 \\ \vdots \\ b_m \end{bmatrix} \tag{2.1}$$

A variety of techniques have been developed to solve linear programming optimization problems. To demonstrate one such elementary technique, consider the optimization problem given in Eq. (2.2).

Objective:

$$maximize\,(2x + 3y)$$

Subject to:

$$\begin{aligned} -3x + y &\leq 0 \\ x - 4y &\leq 0 \\ -x + 2y &\leq 5 \\ x + 2y &\leq 11 \\ 2x - y &\leq 7 \end{aligned} \tag{2.2}$$

In this case, the constraints are listed individually, but since all constraints are inequalities of the same type, they could be expressed as seen in Eq. (2.1). The graphical representation of the feasibility region defined by the constraints is shown in Figure (2.2). As is evident, this region is convex and, as stated previously, must be convex in order to guarantee a unique solution if one exists. This is relatively easy to verify for small systems such as this for which

graphical solutions are available, but can become more challenging for systems of higher dimension. An additional observation of this figure will lead to the realization that when a unique solution exists, it always occurs at a vertex. This suggests that the optimal solution for any linear program can be determined by evaluating the objective function at each vertex of the feasible region as seen in Table 2.1. This observation was made by George Dantzig in 1946 and led to the development of the Simplex algorithm which is widely used to solve problems of this type today. Rather than solving for all vertexes as was done in Table (2.1), the simplex algorithm evaluates the objective function at a single vertex. It then advances along the perimeter of the feasibility region in a strictly increasing or decreasing direction until a maximum or minimum is identified. This approach takes advantage of the convexity of the polytope and will yield poor results if the constraints result in a concavity in the feasibility region.

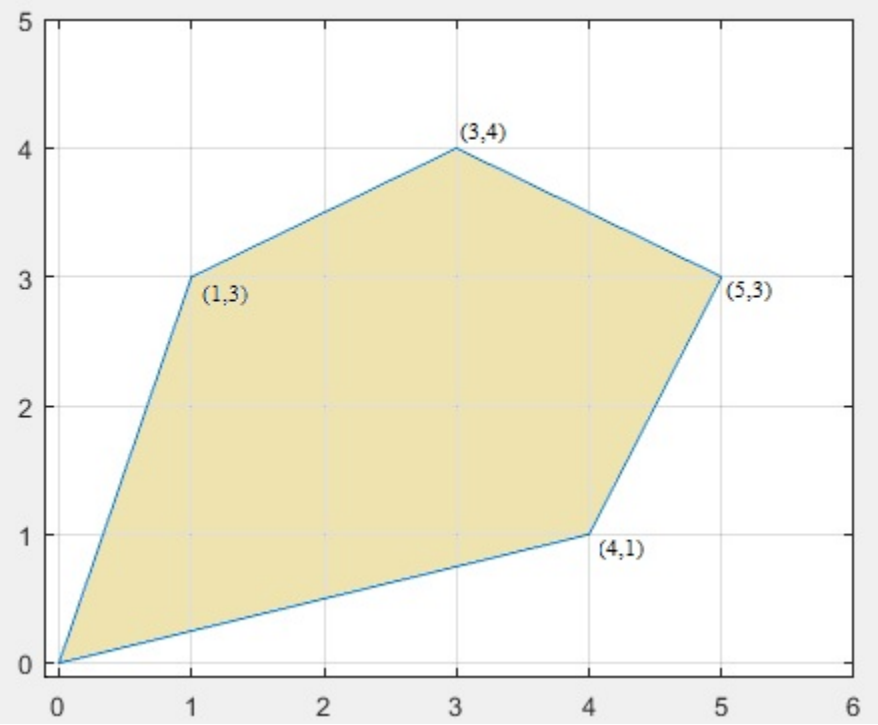

Figure 2.2: Feasible Region for Example Linear Program

To apply linear programming techniques to the problems described in the next three sections, linearity is assumed for each decision variable. Since the system is often non-linear

Table 2.1: Linear Program Solution Table

Vertex	(x, y)	$2x + 3y$
1	$(0, 0)$	0
2	$(1, 3)$	11
3	$(3, 4)$	18
4	$(5, 3)$	19
5	$(4, 1)$	11

as a result of dependencies in the coefficients, the coefficients are evaluated prior to evaluation of the linear program. Specific examples include the coefficients that are determined from fuel consumption function for coal-fired plants and the volumetric flow rate function for hydro-electric generation units which will be introduced in Chapter 3. However, before these are introduced, the microgrid control problem will be introduced and defined in the following sections.

2.2 The Unit Commitment Problem

Unit commitment (UC) is an optimization problem that attempts to optimize the commitment of generation units such that the load is satisfied [9]. This implies that the unit commitment decisions produce binary results corresponding to a committed (on) or an uncommitted state (off) and as such, a subclass of the linear programming model, known as integer linear program, is used. In some cases, such as that of particularly large systems, this problem can be deconstructed into two problems to control the commitment and decommitment separately. In both cases however, the objective of the UC problem is either to minimize cost or to maximize profit. Unit commitment problems formulated to minimize cost are referred to as security constrained unit commitment (SCUC) and include constraints that maintain security in the system by requiring the system to maintain adequate spinning reserve to satisfy sudden changes in demand. As outlined in [14], the typical SCUC problem

is formulated as in Eq. (2.3)

Objective:

$$min \sum_{i=1}^{N_g} \sum_{t=1}^{N_t} \left[C_i \left(P \left(i,t \right) \right) I \left(i,t \right) + S \left(i,t \right) \right]$$

Subject to:

$$\begin{aligned}
&\sum_{i=1}^{N_g} P_G \left(i,t \right) I \left(i,t \right) = \sum_{j=1}^{N_l} P_L \left(j,t \right) && \text{Energy Balance} \\
&\sum_{i=1}^{N_g} r_s \left(i,t \right) I \left(i,t \right) \geq R_s \left(t \right) && \text{Spinning Reserve} \\
&P_{G_{min}} \leq P_G \left(i,t \right) \leq P_{G_{max}}, i \in \{1, N_g\} && \text{Generation Limits} \\
&P_G \left(i,t \right) - P_G \left(i,t-1 \right) \leq R_u \left(i \right) && \text{Ramp Up Constraints} \\
&P_G \left(i,t-1 \right) - P_G \left(i,t \right) \leq R_d \left(i \right) && \text{Ramp Down Constraints}
\end{aligned} \tag{2.3}$$

In the objective function of the SCUC problem, the production cost for the i^{th} unit is represented by $C_i \left(P \left(i,t \right) \right)$ while the $S \left(i,t \right)$ represents the startup costs for the corresponding unit. The decision variables are defined by $I \left(i,t \right)$ and as mentioned previously, are binary states that indicate if the i^{th} unit is committed or decommitted at time t. The constraints force the objective function to choose a solution that adheres to the physics of the system. The energy balance constraint ensures that adequate generation is committed in the system to satisfy the load. In some instances, both the active and reactive components of the complex power are considered as part of the constraints. However as seen here, only the real component of the power is included in this formulation. The second constraint represents the spinning reserve of the system which requires the commitment of units that will maintain a minimum level of spinning reserve to maintain system security. Additional constraints, as shown in eq.(2.3) force the generation to operate within predefined operational limits and limits the rate of change of ramping of thermal units. In addition to the constraints shown, some formulations include fuel, emission, and start up/down time constraints [14] which were not deemed necessary for the application in this thesis and are therefore not specified in the

above formulation.

As an alternate approach to SCUC, unit commitment problems can be formulated to maximize profit. This method is referred to as Price Based Unit Commitment (PBUC) and is commonly used by independent power producers (IPP) in competitive unregulated markets. In this implementation, security does not represent a hard constraint, as maximal profit may result in limiting production or curtailing demand. As a result, the objective function is redefined as a maximization problem and the spinning reserve constraint is relaxed to operate within an upper and lower bound. In addition, PBUC often includes a transmission constraint because transmission congestion can limit the profitability by decreasing an IPP's ability to deliver power to customers. As seen in Eq.(2.4), the formulation for PBUC is similar to that of SCUC:

Objective:

$$max \sum_{i=1}^{N_g} \sum_{t=1}^{N_t} \{\rho_c(i) I(i,t) + \rho_{nc}[1 - I(i)]\}$$

Subject to:

$$\begin{aligned}
&P_{min} \leq \sum_{i=1}^{N_g} P_G(i,t) I(i,t) \leq P_{max} && \text{Energy Balance} \\
&R_{min} \leq \sum_{i=1}^{N_g} r_s(i,t) I(i,t) \leq R_{max} && \text{Spinning Reserve} \\
&P_{G_{min}} \leq P_G(i,t) \leq P_{G_{max}}, i \in \{1, N_g\} && \text{Generation Limits} \\
&P_G(i,t) - P_G(i,t-1) \leq R_u(i) && \text{Ramp Up Constraints} \\
&P_G(i,t-1) - P_G(i,t) \leq R_d(i) && \text{Ramp Down Constraints}
\end{aligned} \tag{2.4}$$

As mentioned previously, the most notable difference between PBUC and SCUC is that formulation of the objective function now chooses to commit or decommit each unit based on the profit function defined by ρ. In this case, ρ_c represents the profit function for committing unit i and ρ_{nc} represents the profit function for decommitting each unit. In addition, the energy balance and spinning reserve constraints now specify a range of operation representing

the region of anticipated profitability. Not shown in this formulation is the transmission congestion constraint which would limit power transmission through congested corridors which was added in the final stages of the simulation development and will be described in Chapter 3.

Since this project sought an integrated approach to the unit commitment and economic dispatch problem, aspects of both the security constrained and price based unit commitment approaches were introduced in the final formulation. The resulting problem was formulated as a minimization problem and therefore most closely follows the security constrained unit commitment problem. Unlike the SCUC approach however, the model did not account for spinning reserve in the system but did specify transmission limits as established in the project master plan. With this in mind, we will now introduce the economic dispatch problem.

2.3 The Economic Dispatch Problem

Economic dispatch has been defined in the Energy Policy Act of 2005 as:

> "the operation of generation facilities to produce energy at the lowest cost to reliably serve consumers, recognizing any operational limits of generation and transmission facilities." [15]

As this definition suggests, the economic dispatch (ED) problem determines optimal utilization of generation resources and shares many similarities to the unit commitment problem discussed in the previous section. In this case however, the optimal dispatch of generation is achieved by minimizing either the fuel consumption or total costs associated with the generation units. In addition, unlike the UC problem that produced binary results, the decision variables for the ED problem represent actual dispatch levels of the generation units expressed either on per unit or proportional bases which allows for traditional linear programming techniques to be used rather than relying on mixed integer techniques.

The following formulation of the ED problem expresses the objective function as a min-

imization of a cost function to allow for integration with the unit commitment and demand response models in Section 2.4. The operating cost function for each unit is represented as the sum of the operating costs which are assumed to be fixed and the fuel costs which are a scalar multiple of the fuel consumption function as seen below:

$$C(i,t) = C_{op}(i) + C_f(i)F(i,t) \tag{2.5}$$

In this formulation, the operating costs $C_{op}(i)$ and the fuel costs $C_f(i)$ are fixed for the i^{th} unit. For thermal units, the fuel consumption function, $F(i,t)$ is defined for the current timestep t between the minimum and maximum generation limits. In the case of hydro-electric generation, the fuel consumption function is replaced with a volumetric flow rate function with similar bounds. Generally, both the fuel consumption function and the volumetric flow rate function are quadratic in nature, however for this study, a linear approximation was used so that existing Matlab tools could be utilized in the simulation.

For large systems, the constraints for the economic dispatch problem are generally minimally defined to ensure convergence to a solution and to decrease solution time. To satisfy the law of conservation of energy, an energy balance constraint is introduced as was done in the unit commitment problem. Additionally, generation limits are placed on each unit to constraint its operational range. These, in conjunction with the objective function, establish the ED problem as seen in [17]:

Objective:

$$min \sum_{i=1}^{N_g} C_i\left(F_i\right)$$

Subject to: (2.6)

$$\sum_{i=1}^{N_g} P_G\left(i,t\right) = \sum_{j=1}^{N_L} P_L\left(j,t\right) \qquad \text{Energy Balance}$$

$$P_{G_{min}} \leq P_G\left(i,t\right) \leq P_{G_{max}}, i \in \{1, N_g\} \quad \text{Generation Limits}$$

To integrate economic dispatch and unit commitment into the single problem statement defined in section 2.5, the objective function will be expressed as a function of the generated power, rather than of the fuel consumption function. This assumes that the power produced is proportional to the fuel consumption when in fact the two share a quadratic relationship. Further, the integrated problem assumes that the generation limits are defined on the interval $[0, 1]\,pu$ when in fact, the lower limit is generally between 25% to 70% of the design capacity [17]. Both of these assumptions were justified given the objectives of the project as defined in Section 1.3. Before formally discussing the integrated model however, a brief introduction to the demand response problem is given in the following section.

2.4 The Demand Response Problem

The demand response (DR) problem often does not refer to a formulative statement as was the case with the economic dispatch and unit commitment problems. Instead, demand response is a set of strategies that can be used to reduce customer demand during peak and off-peak hours. These strategies can include incentives for consumers to use energy efficient devices, implementation of time based pricing schemes, integration of smart technologies that allow direct curtailment of non critical loads, and traditional load shedding techniques. Each of these provide distinct benefits that lower energy consumption both directly and indirectly. As an example, consider the development of the compact fluorescent lamp which reduces energy consumption by 25-80% when compared to a typical incandescent bulb. The compact fluorescent bulbs have a direct impact on energy consumption and so the direct benefit is obvious. What is less obvious however is the increased energy demand associated with production as a result of the extended service life, which can be anywhere from 2 to 20 times that of an equivalent incandescent bulb.

An alternate strategy for demand response was developed in response to the energy crisis of the 1970's that incorporated time based pricing schemes to encourage consumption during

off peak periods. These strategies use a tiered pricing structure that can be dependent on the type of contract that a customer chooses or periodic demand. Demand response clauses allow customers to take advantage of lower utility rates in exchange for curtailment and load shedding agreements for non-critical loads during periods of high demand. In addition, pricing structures based on periodic variability are intended to shift consumer usage to off peak hours where they can take advantage of lower utility rates. This strategy provides the additional benefit of providing some degree of load leveling which can limit the need to ramp up or down thermal generation units. This strategy can also take advantage of smart metering technologies and other smart devices that allow utilities to directly control their operation.

Finally, load shedding and curtailment can be used to remove load from a system when generation does not satisfy demand. This strategy generally uses a priority schedule to select the loads to be curtailed so that non-critical loads are shed before critical loads. In the next section, this approach to demand response will be used because of the high degree of compatibility between it and the early problem statements.

2.5 Integrated Problem Definition

The integrated dispatch algorithm was developed to determine the unit commitment, economic dispatch, and demand response for a microgrid modeled after a moderately sized utility in eastern Idaho that has the ability to purchase power from external sources. In reality, this utility is currently not characterized as a microgrid, however it has significant interest in pursuing energy independence and has worked with Idaho National Laboratory to investigate feasible approaches. This model assumes that the microgrid is capable of expanding generation by adding hydro-electric, wind, solar, and diesel fired generation to satisfy demand when a grid disconnect occurs, but actual hydrological resources are at or near full utilization in the area and the feasibility of adding these generation resources have not been studied.

The initial development of the simulation described in Chapter 4 used a linear cost function dependent on energy production of the generation units instead of a fuel consumption function. This approach provided a close approximation to the quadratic relationship between the variable fuel cost and energy produced, but allowed for the implementation of the problem as an LP which decreased the amount of computational overhead present in the loop structure. This approach carried over as the integrated model was developed since it allowed the objective function for each discrete problem to be of the same form.

Additionally, the early implementation used a traditional approach that evaluated the unit commitment and economic dispatch problems independently. In this case, unit commitment was evaluated for extended periods of time on six hour intervals, while the economic dispatch of the generation units were evaluated on short intervals of 15 minutes. This avoided non-linearity of the system by segregating the commitment and dispatch decisions but introduced significant overhead in the simulation as the result of multiple evaluations per iteration. As a result, iteration cycle times were typically between 50 to 100 milliseconds which was unacceptable since the game resolution was limited to approximately 9000 time-steps per year. In order to reduce the cycle time, the economic dispatch and demand response were integrated into a single mixed integer linear programming problem as in (2.7).

Objective:

$$min \left\{ \begin{array}{l} -\sum_{i=1}^{N_g} C_g\left(i\right) P_g(i,t) \\ -\sum_{j=1}^{N_L} F_L\left(j\right) C_p\left(j\right) P_L\left(j,t\right) \end{array} \right\}$$

Subject to:

$$\begin{array}{ll} \sum_{i=1}^{N_g} P_G\left(i,t\right) = \sum_{j=1}^{N_L} P_L\left(j,t\right) & \text{Energy Balance} \\ P_{G_{min}}\left(i\right) \leq P_G\left(i,t\right) \leq P_{G_{max}}\left(i\right), i \in \{1, N_g\} & \text{Generation Limits} \\ F_L\left(j\right) \in \{0,1\} & \text{Binary Constraint} \end{array} \tag{2.7}$$

For this formulation, the decision variables included the dispatch level of the generation $P_g(i,t)$ on a per unit basis and the binary commitment flag of the loads $F_d(j,t)$. Since renewable generation is assumed to be non-dispatchable, it only serves as inputs to the energy balance equation and does not appear in the objective function. To prevent the model from choosing to shed load rather than ramp generation, a penalty cost $C_p(j)$ was assigned to the load shed decision variables that artificially represented the loss of revenue and customer satisfaction. This also includes the energy from spot market purchases P_{sm} and the change in the energy storage ΔP_{ST}. Critical loads such as hospitals were assigned the highest penalty cost and non-critical loads where assigned the lowest. This implementation retained a lower generation limit of 50% for both thermal and hydro-electric units. As a result of implementing this approach independent of the unit commitment problem, the desired cycle time was reduced to less that 1 millisecond, which allowed the simulation to evaluate approximately one year of data in 15 minutes.

Objective:

$$min \left\{ \begin{array}{l} -\sum_{i=1}^{N_G} C_G\left(i\right) P_G(i,t) \\ -\sum_{j=1}^{N_L} F_L\left(j\right) C_p\left(j\right) P_L\left(j,t\right) \\ +C_{sm}P_{sm} + C_s\Delta P_{ST} \end{array} \right\}$$

Subject to:

$$\begin{array}{ll} \sum_{i=1}^{N_g} P_G\left(i,t\right) + P_{sm} + \Delta P_{ST} = \sum_{j=1}^{N_d} P_L\left(j,t\right) & \text{Energy Balance} \\ 0 \leq P_G\left(i,t\right) \leq P_{G_{max}}\left(i\right), i \in \{1, N_g\} & \text{Generation Limits} \\ P_{SM} \leq P_{TL} & \text{Transmission Limit} \\ 0 \leq P_{ST} \leq P_{ST_{max}} & \text{Storage Constraint} \\ F_L\left(j\right) \in \{0,1\} & \text{Binary Constraint} \end{array} \tag{2.8}$$

The integration of the unit commitment problem into this framework proved to be somewhat challenging. When implemented directly into the objective function as a binary constrained

decision variable as was done for the demand response, the system became non-linear. To resolve this issue, the unit commitment was implemented as a relaxation of the generation limit constraints. This approach limits the realism of the model for thermal units, but allowed the system to retain the desired simulation speed. In addition, to allow for power to be imported and storage to be included in the system, eq.(2.7) was modified to include storage, ramp rate restrictions and transmission constraints as seen in Eq. (2.8). With the formulation of the integrated dispatch algorithm in place, the definition of the model inputs was developed which are described next in Chapter 3.

Chapter 3: Definition of System Inputs

The development of the integrated dispatch algorithm provides a generalized platform capable of scaling to large systems and is primarily limited by the computational power of the microprocessor. It allows for a variety of generation and load elements, each with unique attributes, to serve as inputs while also constraining the problem by imposing generation ramp rate limits, storage limits, transmission line limits, and energy conservation in the system. This provides the opportunity to include many types of generation and load models in the simulation, but to limit the scope of the project, only those types that are representative of a broad class of elements were included. As an example, generation was categorized as renewable, dispatchable, and spot market energy purchases in the event that local energy supply does not satisfy demand. In the case of the load in the system, each load type was segregated into either residential, commercial and industrial types. In addition, while electric vehicle charging system models are still in the developmental stages, loads from these systems are included to stress the model. Grid scale storage is represented in the system in a coupled source/sink configuration and is assumed to be locally available for energy storage. The models for each of these microgrid inputs will be developed in the following sections.

3.1 Renewable Generation Models

Renewable generation is available from a variety of sources which include wind, solar, hydroelectric, geothermal, and biomass sources. Of these, only the first three are modeled in the project since they represent the majority of investment in renewable energy and are prevalent in the Pacific Northwest. Each of these renewable resources are assumed to be non-dispatchable and non-curtailable, which serves to demonstrate the challenges faced when integrating renewable resources into a power system. Because of this, the renewable resources are only constrained by the peak capacity of the resource and not by the integrated dispatch algorithm. The renewables therefore do not appear in the objective function of the integrated dispatch algorithm and only appear in the energy balance constraint as part of

the total available generation. In the event that an independent power producer chooses to significantly increase the penetration of renewable resources in the microgrid, the opportunity for significant variability in total generation capacity is possible since these resources cannot be curtailed. The formulation of the renewable models follows in the following sections.

3.1.1 Solar Energy Model

The energy from the available solar resources was determined by normalizing the measured solar radiation incident to the surface of the solar array. This measurement was preferred over other data sources because it accurately represented daily and seasonal solar variability. In addition, the data-set includes variability as the result of cloud cover and other inclement weather conditions which adds additional realism to the simulation. This data-set was collected from the National Solar Radiation Database [18] which is maintained by the Renewable Resource Data Center (RRDEC) at the National Renewable Energy Laboratory (NREL). The renewable energy available from solar installations is defined in Eq. (3.1) for the n^{th} timestep.

$$G_{RS}\left(n\Delta t\right) = N_s P_s \Delta t \frac{H_s\left(n\Delta t\right)}{max\left(H_s\right)} \tag{3.1}$$

This formulation assumes that all solar installations have a maximum power capacity P_s. The number of solar arrays available N_s is specified by the user to allow for different degrees of solar penetration in the microgrid. The measured solar radiation H_s is from the data-set for the specified timestep and is normalized to the maximum annual solar radiation. This normalization process allows for scaling of the generation as additional solar resources are brought online while maintaining the short and long term periodic variability in the data-set.

3.1.2 Wind Energy Model

The energy from the available wind resources was determined by approximating the characteristic power curve of the Vestas V110 2 MW wind turbine [19] which has characteristics typical of wind turbines of comparable size as seen below in Figure 3.1. The figure shows the turbine has a cut-in speed of 3 meters per second and reaches full production for wind speeds between 12 and 20 meters per second.

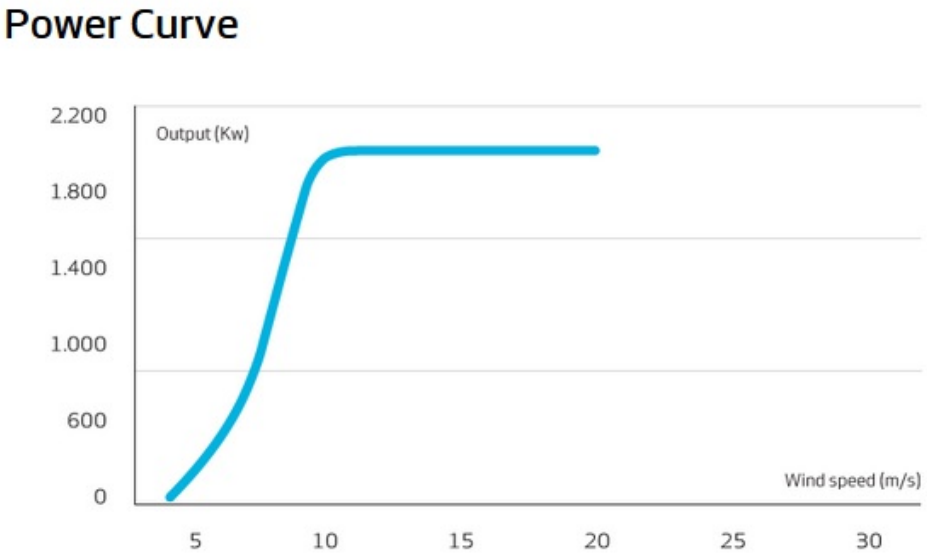

Figure 3.1: Vestas V110-2MW Power Curve [19]

From this, the energy available from the wind resources was defined as a piece-wise linear function as in Eq.(3.2) that approximates this power curve characteristic. Similar to the energy calculation for solar energy model, the wind energy model assumes that all wind turbines share the same characteristic and therefore the peak available power is determined by the product of the peak available power per unit P_w and the total number of units N_w.

$$G_{RW}\left(n\Delta t\right) = \begin{cases} N_W P_W \Delta t \frac{\nu_W\left(n\Delta t\right)}{9}, & 3 < \nu_W\left(n\Delta t\right) \leq 12 \\ N_W P_W, & 12 < \nu_W\left(n\Delta t\right) \\ 0, & otherwise \end{cases} \tag{3.2}$$

The wind speed data ν_w, was collected from the System Advisory Model [20] developed by the National Renewable Energy Laboratory and represents wind speed data collected at Idaho Falls Regional Airport. The data was collected on an hourly bases. It was therefore necessary to interpolate the sub-hour datapoints within this data-set to provide the 35,040 points of data required for the simulation. Similar to the solar energy model, significant challenges are presented to the independent power producer if the penetration of wind energy becomes substantial.

3.1.3 Hydro-Electric Energy Model

The energy from the available hydro-electric resources was formulated in a similar manner to that of the solar resources as seen in Eq. (3.3). In this case however, the volumetric flow rate used in the formulation rather than the solar radiation to determine the energy available from the resource. The volumetric flow rate data-set represents historical flow rate data for the Snake River which was collected by Idaho Falls Power and the Center for Advanced Energy Studies [21] with sampling performed at 15 minute intervals. The volumetric flow rate data-set was normalized to the peak flow rate in the data-set and scaled to the number of Hydro-Electric installations selected by the independent power producer and assumes a common peak power capacity of each installation.

$$G_{RH}\left(n\Delta t\right) = N_{RH} P_{RH} \Delta t \frac{Q_{RH}\left(n\Delta t\right)}{max\left(Q_{RH}\right)} \tag{3.3}$$

This model does not account for over utilization of the hydro-geological resources and therefore can misrepresent the total available power from these resources. However, unlike energy from solar and wind, higher penetration of hydro-electric generation, which experiences relatively long term seasonal variability, does not present a significant challenge when integrating into the dispatch model.

3.2 Dispatchable Generation and Spot Market Contracts

Dispatchable generation refers to generation sources that are available to a system operator which can be dispatched to satisfy the electrical load in a system. In the context of this project, dispatchable generation represents the local generation sources that the independent power producer has direct control of and includes local gas-fired generation, coal-fired generation, and hydro-electric generation facilities. In this case, the dispatchable hydro-electric generation is distinguished from renewable hydro-electric generation discussed previously by assuming that dispatchable hydro-electric sources have adequate storage available to allow for some degree of spinning reserve to be provided by the resource. In the case of hydro-electric sources classified as renewable, these sources are considered to be run of the river, which implies that they have no storage available and prevents them from being considered dispatchable.

Since the dispatchable generation sources are controlled by the integrated dispatch algorithm, no data is required from data-sets as seen in Eq. (3.4). Similar to the other models, it determines the peak energy capacity of the respective sources given the number of units available and the peak power output of each unit. The integrated dispatch algorithm then determines the optimal dispatch level, $d_{\{C,G,H\}}(n\Delta t)$, for the current timestep, where the dispatch level is defined on the interval $[0, 1]$ and constrained by the ramp rate limits assigned to the particular generation type and the energy balance equation.

$$G_{D\{C,G,H\}}(n\Delta t) = \left(N_{\{c,g,h\}} P_{\{c,g,h\}} \Delta t\right) d_{\{c,g,h\}}(n\Delta t) \tag{3.4}$$

The energy available from spot market purchases is similarly formulated as seen in Eq. (3.5) and allows for energy to be purchases from external sources that are assumed to be ideal. The energy from spot markets assumes that N_{SM} contracts have been purchased and that any portion of the total energy available may be used. Because of this, the decision variable d_{SM} is defined on the interval $[0, 1]$ as was the case for the dispatchable generation.

Unlike the dispatchable energy model however, the energy purchased from spot markets does not have a ramp rate limit imposed since the energy is assumed to be pre-allocated by the contract. This allows the integrated dispatch algorithm to choose any dispatch level and prevents ramp rate restriction of the dispatchable generation or variability in renewable generation from violating the energy balance constraint.

$$G_{SM}\left(n\Delta t\right) = \left(N_{sm} P_{sm} \Delta t\right) d_{sm}\left(n\Delta t\right) \tag{3.5}$$

3.3 Load Models

Loads are commonly segregated into segments of the distribution system that predominantly service residential, commercial, and industrial customers. Each of these segments may be curtailable depending on the design of the distribution system and can include critical loads. While electric vehicle charging systems are commonly included in one or more of these load segments, they are implemented separately so that the performance of the integrated dispatch algorithm can be evaluated for different levels of penetration. The demand response strategy implemented by the utility generally includes provisions for load shedding in the event that generation cannot adequately meet the demand of the load. The models that follow assume that the microgrid has such provisions and determines if one or more of the loads must be shed to maintain system stability. Each of the loads included in this project are described in the next two sections.

3.3.1 Primary Load Models

The primary load models represent the residential, commercial and industrial loads which are assumed to be aggregate models of distribution feeders servicing each of these load types and assumes that load sheddding provisions exist for each load type. Each of the primary loads display periodic daily behavior and therefore tend to be relatively simple to

include into a dispatch algorithm. For this study, the residential and commercial load models use data-sets derived from the the System Advisory Model [20] which are constructed from average historical demand profiles for population centers that share common characteristics as the study area. The data-set for industrial loads are derived from data collected by the Center for Advanced Energy Studies [21] and represents actual historical load demand from a distribution feeder serviced by Idaho Falls Power that primarily services an industrial zone. Each element from these data-sets, represented by $Y_{\{R,C,I\}}(n\Delta t)$, is normalized and multiplied by the peak energy demand of the corresponding load as seen in Eq. (3.6). The demand response flag, $d_{\{R,C,I\}}$, is defined on the set $\{0,1\}$ and represents the binary decision variable determined by the integrated dispatch algorithm that indicates if the load is active or inactive.

$$L_{\{R,C,I\}}(n\Delta t) = \left(N_{\{r,c,i\}} P_{\{r,c,i\}} \Delta t\right) \frac{Y_{\{r,c,i\}}(n\Delta t)}{max\left(Y_{\{r,c,i\}}\right)} d_{\{r,c,i\}}(n\Delta t) \tag{3.6}$$

To force the integrated dispatch algorithm to prefer to ramp generation rather than shed load, a penalty cost was assigned to loads in the objective function which represents both the cost of lost revenue and customer satisfaction. As will be seen in Chapter 4, the penalty cost provided a mechanism to tune the behavior of the integrated dispatch algorithm.

3.3.2 Electric Vehicle Load Models

Electric vehicle charging systems are unique in that they can represent significant, non-periodic loads on the electrical grid. While some periodicity can be assumed for residential based charging systems that schedule the recharge cycle, Table 1.1 shows that these loads are typically less that 7 kW and therefore not likely to present significant challenges to a microgrid operator or distribution system. Further, since these loads will likely occur in the evening, some degree of daily load leveling can be assumed. The commercially installed electric vehicle charging systems however are anticipated to present significant challenges

both to microgrids and the larger electrical grid as a whole as a result of the high power requirements of up to 120 kW over very short intervals. Since these systems will likely be used predominantly in preparation for the return commute, significant loading will occur during peak demand periods that could be difficult to distinguish from system fault conditions.

Electric vehicle charging loads were modeled separately from the primary load types to allow the system operator the option to investigate the impact of increased electric vehicle penetration. While these loads will be included as part of distribution feeders that aggregately represent the types of loads previously introduced in the last section, it is likely that individual metering and control will be possible since these charging systems often feature smart metering technology. Currently however, the impact of these types of loads have not been extensively researched. While efforts have attempted to develop representative models [22], many have not been widely accepted. Because of this, the electric vehicle charging loads were determined for the product of the nominal load per charger type and a uniformly distributed variable $n_{EV\{r,c\}}$.

$$L_{EV\{R,C\}}\left(n\Delta t\right) = \left(n_{EV\{r,c\}} P_{EV\{r,c\}} \Delta t\right) d_{EV\{r,c\}}\left(n\Delta t\right) \tag{3.7}$$

Where:

$$n_{EV\{r,c\}} \in \left\{0, 1, ..., N_{EV\{r,c\}}\right\} \tag{3.8}$$

The number of electric vehicle charging systems active during any iteration of the simulation is determined at the beginning of the iteration for inclusion into the integrated dispatch algorithm evaluation. This provided dynamic loading of the system in terms of these charging systems which provides a reasonable approximation for the commercially installed systems since the charging period roughly corresponds with the selected timestep of the simulation. In the case of the residential based units however, Table 1.1 indicates that the charge times can be in excess of 12 hours. Therefore, this approach needs to be refined to provide a more accurate representation of these systems.

3.4 The Energy Storage Model

While grid scale storage is still prohibitive both economically and technologically, energy storage was included in the simulation as an optional element of the microgrid that can be added by the system operator. The model used to represent energy storage assumes that the change in storage, ΔST, is a result of the excess or deficient energy in the microgrid. As such, the change in storage is represented in the integrated dispatch algorithm as the difference between the discharging, ST_{source}, and charging, ST_{sink}, state of the storage element. These elements are modeled in the same manner as generation and load elements, but require separate coupling and state of charge constraints to be added that ensure that the rate of charge is limited and that charge and discharge do not occur simultaneously. This allowed the change in storage to be formulated as seen in Eq. (3.9).

$$\Delta ST = ST_{sink} - ST_{source} \tag{3.9}$$

The state of charge of the energy storage element is evaluated after the optimal change in storage is determined for each iteration. The state of charge is defined in Eq. (3.10).

$$ST_{SOC}\left(n\Delta t\right) = ST_{SOC}\left(\left(n-1\right)\Delta t\right) - \Delta ST \tag{3.10}$$

This implementation allowed the change in storage to be implemented directly into the objective function and energy balance equation of the integrated dispatch algorithm. The state of charge of the energy storage model was evaluated after the integrated dispatch algorithm determined the optimal change in storage allowed for additional constraints to be placed on the storage element to define minimum and maximum storage levels.

Chapter 4: Simulation Development

The simulation developed to test the integrated dispatch algorithm was created in MATLAB® R2015b and uses functionality from the Optimization Toolbox™, which provides several tools useful for optimization problems such as those presented in Chapter 2. The simulation requires two input parameters designated as N_g and N_l which are single dimensional arrays containing the number of generation and load elements as defined in Chapter 3. The function begins by initializing and importing the data-sets and then iteratively evaluates the integrated dispatch algorithm until the end of data is reached. The flowchart shown in Figure 4.1 illustrates the high level structure of the simulation. A complete listing of the simulation code is available in Appendix A.

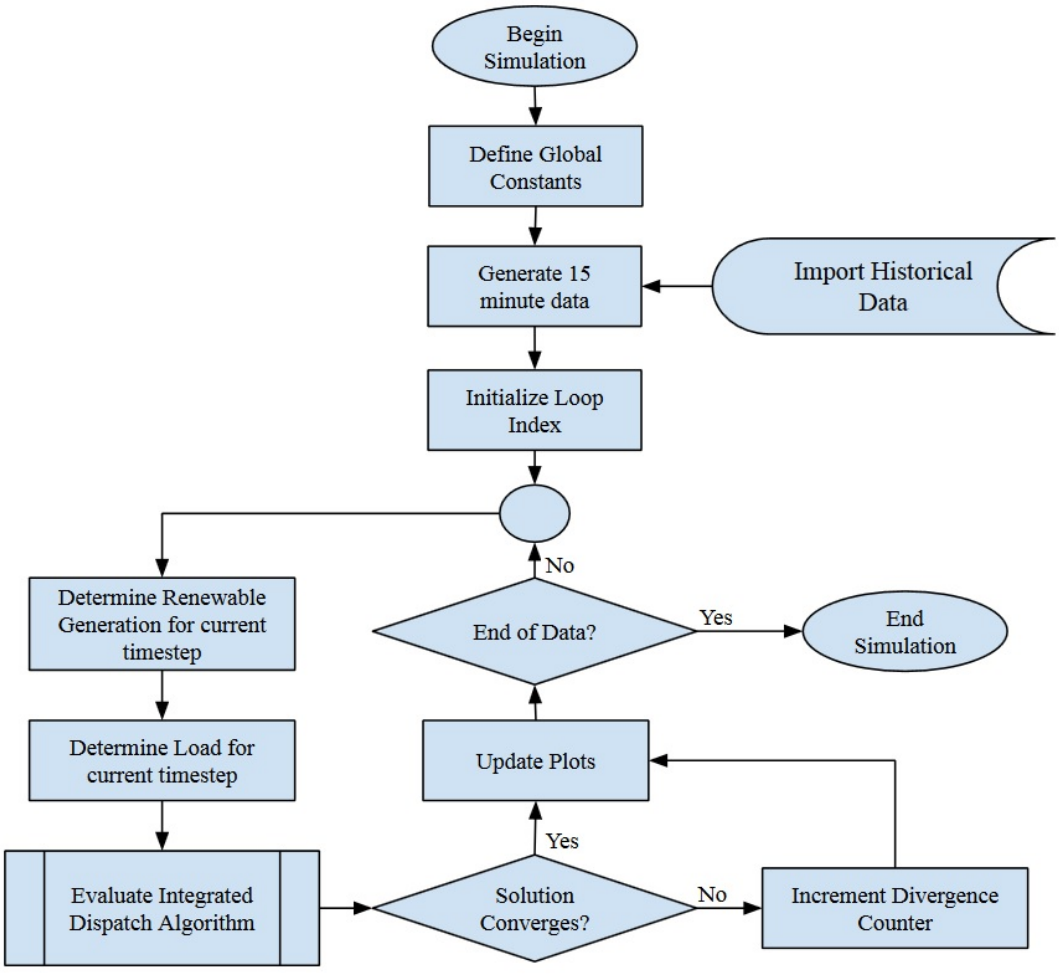

Figure 4.1: Simulation Flowchart

In the following sections, the simulation will be divided into three primary areas that include the data initialization, the implementation of the integrated dispatch algorithm, and error handling of the data. Each of these sections will describe the formulation and implementation of the integrated dispatch model developed in Chapter 2 as well as the generation and load models described in Chapter 3.

4.1 Data Initialization

The data initialization section of the code includes the declaration of the global constants and data structures used within the simulation. In addition, the historical data-set used by the renewable generation and load models is imported from the external sources and utilized to generate the 15 minute data-set.

The simulation defines two global constants represented by scalar quantities that include the simulation timestep and the width of the plot window, labeled *dt* and *plotwidth* respectively. In addition, the data structures defined for the generation, load, and storage models contain static parameters that are passed within the structures to the functions that require them. These static parameters are summarized in Tables 4.1, 4.2 and 4.3.

4.1.1 Data Structure Initialization

There are three data structures in the simulation that store static and dynamic data for the generation, load, and storage elements of the simulation. Each structure is represented by an mxn array using a similar syntax so that data can be easily interpreted. As the name suggests, these arrays were initially implemented as structures, however the manner that these structures are implemented in Matlab presented challenges when storing dynamic data; therefore, array elements were used instead.

The generation data structure is represented by an $8x10$ array arranged such that the rows represent the specific generation types as described in Chapter 3 while the column definitions

are described in Table 4.1. Several of the parameters within this array are reserved for future implementation and are currently not implemented in the simulation. These include the maximum number of units allowed in the simulation and the start up cost associated with starting or restarting a coal or gas-fired generator.

Table 4.1: Generator Data Structure

Column	Name	Associated Variable	Type
1	Number of units	$N_{\{s,w,rh,g,c,h,sm\}}$	Input Parameter
2	Max Number of units		Reserved
3	Peak power per unit	$P_{\{s,w,rh,g,c,h,sm\}}$	Static Parameter
4	Ramp up rate (MW/dt)		Static Parameter
5	Ramp down rate (MW/dt)		Static Parameter
6	Fuel Cost (USD/MWhr)	$C_{f\{s,w,rh,g,c,h,sm\}}$	Static Parameter
7	Start Up Cost (USD)		Not Implemented
8	Operations Cost (USD/MWhr)		Static Parameter
9	Instantaneous Value (MWhr)	$G_{\{R,D,SM\}\{S,W,H,G,C\}}$	Dynamic Parameter
10	Percent dispatched	$d_{\{c,g,h\}}$	Dynamic Parameter

The load data structure is represented as an $7x8$ array and is similarly constructed so that the first six rows represent the different types of loads discussed in Chapter 3. The seventh row is included to allow for system faults and is represented as an instantaneous $250MW$ load on the system. This mechanism was included for later implementations and therefore serves as a placeholder for future development. The column definitions for the load data structure are seen in Table 4.2.

Table 4.2: Load Data Structure

Column	Name	Associated Variable	Type
1	Number of units	$N_{\{r,c,i,EVr,EVc\}}$	Input Parameter
2	Max Number of units		Reserved
3	Peak demand (MW)	$P_{\{r,c,i,EVr,EVc\}}$	Static Parameter
4	Energy Cost (USD/MWhr)	$C_{\{r,c,i,EVr,EVc\}}$	Static Parameter
5	Penalty Cost (USD/MWhr)	$C_{P\{r,c,i,EVr,EVc\}}$	Static Parameter
6	Load Shed Preference		Not Implemented
7	Instantaneous Value (MWhr)	$L_{\{R,C,I,EVR,EVC\}}$	Dynamic Parameter
8	Unit Commitment Flag	$d_{\{r,c,i,EVr,EVc\}}$	Dynamic Parameter

The storage data structure is represented by a $3x8$ array, where the rows represent the storage source element, storage sink element, and the grid storage state of charge. While the state of charge element was not required to be included in this array, it was included to provide a similar implementation for all three components. In addition, the storage elements include charge and discharge characteristics which were incompatible with the generation and load data structures. Table 4.3 shows the column definition for the storage data structure.

Table 4.3: Storage Data Structure

Column	Name	Associated Variable	Type
1	Number of units	N_{ST}	Input Parameter
2	Max Number of units		Reserved
3	Storage Capacity/unit (MW)	P_{ST}	Static Parameter
4	Charge/Discharge Rate (MWhr/dt)		Static Parameter
5	Charge/Discharge Cost (USD/MWhr)	C_{ST}	Static Parameter
6	Operation Cost (USD/MWhr)	C_{OST}	Static Parameter
7	Instantaneous Value (MWhr)	ST_{SOC}	Dynamic Parameter
8	Change in charge (MWhr)	ΔST	Dynamic Parameter

4.1.2 Imported Data Initialization

Data-sets were imported for both the renewable energy and load profiles. The data-sets used for the renewable energy and industrial load profiles represent historical data while the residential and commercial load profiles were generated from models developed by the National Renewable Energy Laboratory as described in Chapter 3. The solar radiation data was accessed directly from the solar radiation database available from NREL [18] which was collected hourly. The residential and commercial data was similarly collected from an hourly dataset from the System Advisory model [20]. This data was linearly interpolated to produce the quarter hour and half hour data points which resulted in 35,040 data points per year for each data-set and stored into $FifteenMinuteData$ array. Figure 4.2 illustrates the algorithm used to interpolate the data.

The historical data-sets for wind speed, flow rate, and industrial load were collected on

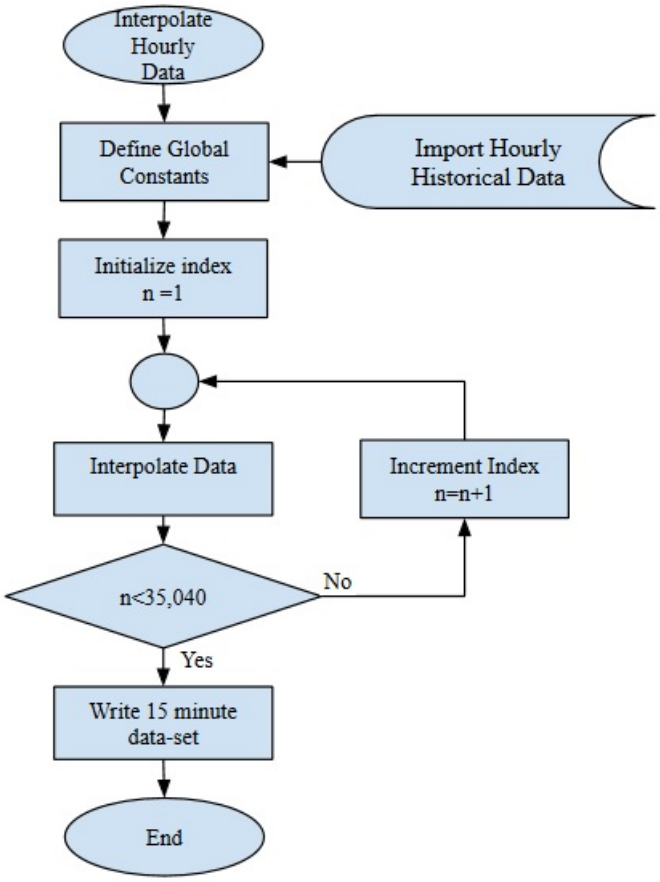

Figure 4.2: Interpolation Algorithm Flow Chart

10 minute intervals by the Center for Advanced Energy Studies [21]. The data was imported into a spreadsheet format and interpolated for the fifteen minute data points using a modulus operation which resulted in the 35,040 data points representing one year's worth of data. This data was similarly stored in the $FifteenMinuteData$ array for use within the iterative loop which is summarized in Table 4.4.

4.2 Integrated Dispatch algorithm Implementation

The integrated dispatch algorithm was implemented using the MATLAB® function *intlinprog* which is included in the Optimization Toolbox™. This function evaluates mixed integer linear programming problems and requires at least three parameters that define the objective function and constraints of the problem. The general format of the function is seen

Table 4.4: Storage Data Structure

Row	Data-set	Data Source	Description
1	Solar Radiation	NREL	Interpolated from hourly data
2	Wind Speed	CAES	Interpolated from 10 minute data
3	Normalized Hydro	CAES	Interpolated from 10 minute data
4	Normalized Residential	NREL	Interpolated from hourly data
5	Normalized Commercial	NREL	Interpolated from hourly data
6	Normalized Industrial	CAES	Interpolated from 10 minute data

in Eq. (4.1).

$$intlinprog\left(f, \text{intcond}, A, b, Aeq, beq, lb, ub\right) \tag{4.1}$$

The function f was formulated as a $1x12$ array containing the coefficients of the objective function as formulated in Eq. (2.8). The inequality constraints which included the generation and transmission limits and storage constraints were included in a $9x12$ coefficient matrix A and a $9x1$ constant array b which were expressed in the general form as seen in Eq. (2.1). The equality constraint included only the energy balance constraint which was represented as a $1x12$ coefficient matrix Aeq and a scalar quantity represented by beq. Since only the load demand response flags were defined as integer quantities, the integer condition vector *intcon* included references to each of the associated decision variables. Finally, the lower and upper bound for each decision variable was defined by the lb and ub arrays.

4.2.1 Error Handling and Convergence Testing

In addition to the solution, the *inlinprog* function returns an *exitflag* which was used for error handling and convergence testing in the simulation. Under normal conditions, the function will return an exit flag of 1 to indicate that a convergent solution was achieved. In the event that exit flag is not equal to 1, a counter, which is initialized to zero, is incremented. This provided a mechanism to identify the number of non-feasible solutions and the rate of divergence of the simulation.

Chapter 5: Results

The results of this research are discussed in the following two sections. Section 5.1 presents the results as published in Proceedings of the 2016 IEEE Conference on Technologies for Sustainability and presents evidence of the convergence of the integrated dispatch algorithm. Section 5.2 expands on the results by introducing the simulation behavior under additional conditions.

5.1 IEEE Technologies for Sustainability Conference Publication

The results of this project were published in the fourth annual IEEE Technologies for Sustainability Conference (SusTech 2016) and are reprinted here following the specified formatting requirements of the College of Graduate Studies. the numbers for all citations, equations and tables have been updated for inclusion in this thesis and therefore differ from the publications originally accepted form. The original paper is available upon request.

Dispatch Control with PEV Charging and Renewables for Multiplayer Game Application

Nathan Davis, Student Member, IEEE, Brian Johnson, Senior Member, IEEE, Timothy McJunkin, Senior Member, IEEE, Don Scoffield, Sera White

ABSTRACT:

This paper presents a demand response model for a hypothetical microgrid that integrates renewable resources and plug-in electric vehicle (PEV) charging systems. It is assumed that the microgrid has black start capability and that external generation is available for purchase while grid connected to satisfy additional demand. The microgrid is developed such that in addition to renewable, non-dispatchable generation from solar, wind and run of the river hydroelectric resources, local dispatchable generation is available in the form of small hydroelectric and moderately sized gas and coal fired facilities. To accurately model demand,

the load model is separated into independent residential, commercial, industrial, and PEV charging systems. These are dispatched and committed based on a mixed integer linear program developed to minimize the cost of generation and load shedding while satisfying constraints associated with line limits, conservation of energy, and ramp rates of the generation units. The model extends a research tool to longer time frames intended for policy setting and educational environments and provides a realistic and intuitive understanding of beneficial and challenging aspects of electrification of vehicles combined with integration of green electricity production.

Index Terms: Plug in electric vehicle, demand response, real time dispatch, gamification.

I. INTRODUCTION:

The introduction of charging stations for plug-in electric vehicles (PEVs) is intended to decrease greenhouse emissions by relying on bulk power generation rather than internal combustion engines for short to medium length commutes. This will inherently increase the load on the power grid and has the potential to stress existing distribution feeders, but can be beneficial if the charging cycles are scheduled during off peak hours. This is supported by studies that suggest that load leveling is positively impacted if residential charging occurs during the off-peak hours from midnight to 6:00 AM [22]. The impact of publicly accessible direct current fast charging systems (DCFC) is less well understood but they are anticipated to be used on the reverse commute and, as a result, increase the burden on the power grid during peak-load hours. To further complicate the issue, renewable generation from photovoltaic and wind technologies are inherently intermittent and, without storage, cannot be relied upon for demand response.

In this regard, various authors have developed models to solve the dispatch and commitment problems for PEV charging systems and renewable resources when considered in isolation [23][24]. However, there is a need to develop a demand response model that incorporates these elements while providing reliable dispatch to satisfy the energy balance equation.

This paper proposes a model formulated as a mixed integer linear program that incorporates generation from renewable and dispatchable resources, energy from contract markets and grid scale storage, and load shedding decisions for distribution feeders servicing residential, commercial, and industrial loads. While PEV charging systems have been aggregated into these loads in some studies, the model described in this paper integrates them separately and discretely with the assumption that they can be remotely curtailed for load shedding purposes. The model defines the objective function as a cost function associated with unit dispatch and commitment of local generation and load resources while satisfying the constraints associated with energy conservation and equipment rating limitations. This model is used to demonstrate the dynamic response of the system to variability of the renewable generation and the increased demand on the system by the PEV charging systems. These are then aggregated into the energy balance equation and used to minimize the cost of the dispatchable resources for the current time step. This model is applied to extend a multi-player game simulation of microgrids [11] to extended time frames for exploration of greater transportation electrification.

This paper is arranged as follows. Section II specifies the scope and assumptions of the proposed work. It is followed in Section III by a description of the model development. Section IV provides a summary of the results followed by the conclusion in Section V.

II. SCOPE:

The model presented in this paper is limited to a single hypothetical microgrid acting independent of surrounding utilities. External generation may be purchased on spot markets from polluting and non-polluting sources which are represented by infinite buses constrained only by the contract amount. The generation and load models were developed from historical and stochastic sources in order to demonstrate the dynamic behavior of the demand response model for determining the optimal dispatch of the local resources. Further, the simulation has been developed with the flexibility to allow for system faults but has not integrated them at this time. Finally, in order to demonstrate the challenges associated with renewable

resource integration into power systems, the renewables are assumed to be non-curtailable and therefore are always connected to the microgrid after installation. Finally, to allow for adequate fidelity and compatibility with DCFC system charge times, the simulation is developed for a medium time scale simulation that uses a time step of 15 minutes to represent the primary loading periods of the day in order to approximate the response of the model to variable renewable generation and PEV charging systems.

III. MODEL DEVELOPMENT:

The objective of the study is to develop a demand response model that can be used to determine the optimal dispatch of the local dispatchable generation resources and perform load shedding as needed to maintain energy balance when renewable generation variation is non-curtailable. To accomplish this, the model allows for grid-scale energy storage and for purchase decisions from spot markets. In order to achieve these objective, three primary aspects were developed to demonstrate this principle:

A. *The Generator Model*

The generation model considers three primary contributions to total generation. These include local renewable generation, local dispatchable generation and energy purchased and imported from spot markets. Each generation resource is assigned an operation cost, a fuel cost, and a ramping cost. Local renewable generation cannot be curtailed and represents distributed generation within the microgrid. The costing structure assigns no fuel or ramping cost to renewable resources, but assigns high operating costs, which, in this case, is used to represent the capital and regulatory contract costs. The three types of renewable generation include solar, wind, and run of the river hydro-electric. The solar generation model uses normalized normal incident radiation data collected by the Renewable Resource Data Center (RREDC) at the National Renewable Energy Laboratory (NREL) [8]. This dataset was selected because it accounted for output variations as a result of climatic, geographic and seasonal characteristics. The wind generation model uses hourly wind speed datasets from

the System Advisory Model (SAM) developed at NREL [18] which was interpolated to satisfy the desired time step selected for the model. The energy output produced from the wind resources was defined using the characteristics of the Vestas V110 2MW turbine [19]. The run of the river hydroelectric generation model was developed by normalizing historical volumetric Snake River flow rate data sampled at 15 minute intervals provided by Idaho Falls Power [21] and interpolating for the simulation time step, as required.

The renewable energy generation for each resource, expressed in units of MWhrs, is expressed in Eq. (5.1).

$$
\begin{aligned}
G_{RS}\left(n\Delta t\right) &= N_s P_s \Delta t \frac{H_s\left(n\Delta t\right)}{max\left(H_s\right)} \\
G_{RW}\left(n\Delta t\right) &= \begin{cases} N_w P_w \Delta t \frac{\nu_W\left(n\Delta t\right)}{9}, & 3 < \nu\left(n\Delta t\right) \leq 12 \\ N_w P_w, & 12 < \nu\left(n\Delta t\right) \\ 0, & otherwise \end{cases} \\
G_{RH}\left(n\Delta t\right) &= N_H P_H \Delta t \frac{Q_H\left(n\Delta t\right)}{max\left(Q_H\right)}
\end{aligned}
\tag{5.1}
$$

Where:

$$
\begin{aligned}
G_{R\{S,W,H\}} &\rightarrow \text{Generated Renewable energy (MWhr)} \\
N_{\{S,W,H\}} &\rightarrow \text{Total number of units} \\
P_{\{S,W,H\}} &\rightarrow \text{Peak Power output (MW)} \\
H_S &\rightarrow \text{Solar Irradiance } \left(\tfrac{W}{m^2}\right) \\
\nu_w &\rightarrow \text{Wind Speed } \left(\tfrac{m}{s}\right) \\
Q_H &\rightarrow \text{Volumetric Flow Rate } \left(\tfrac{m^3}{s}\right) \\
\Delta t &\rightarrow \text{timestep (s)} \\
n &\rightarrow \text{index}
\end{aligned}
$$

Note: a linear approximation of wind generation from minimum to name plate (maximum) power from the cut in wind speed of 3m/s to peak generation wind speed of 12m/s for the Vestas turbine. The cut off speed at which the turbine shuts down operation is 20m/s.

Local dispatchable generation is assumed to exist within the microgrid and represents

fixed assets that can be dispatched at any level between 0 and 100%. The costing structure for dispatchable resources includes operational, fuel, and ramping costs. In addition, asymmetric ramp up and ramp down rates are associated with each dispatchable resource to realistically limit the rate at which the resource can respond to load changes. The three types of dispatchable generation include coal fired generation, gas fired generation, and hydroelectric generation. Coal fired generation incurs the highest ramp cost and lowest ramp rate while hydro-electric resources incurring the lowest ramp cost, no fuel cost and highest ramp rate. For the purpose of this paper, limits on the availability of feedstock (e.g. coal, natural gas, and stored water) are not considered.

Energy purchased from spot markets is limited to a predefined upper boundary defined by the purchased contract. The energy is assumed to be delivered from an infinite bus and therefore is not constrained by ramp rate restrictions. Since energy purchased from spot markets is assumed to be external to the microgrid, it is subject to transmission line limits and losses. While not implemented at this time, future implementations will allow for day ahead energy contracts. For this reason, any amount of energy may be purchased on each timestep within the predefined limits. However, because of restrictive pricing associated with the spot markets, preference is always given to fully utilize the local dispatchable resources before utilizing spot markets. Variable pricing in the spot market can be implemented given a specification of a model of the market or multiplayer game interaction.

The peak energy capacity of local dispatchable generation resources and spot market contracts are similarly modeled and are of the form:

$$\begin{aligned} \left|G_{D\{C,G,H\}}\right| &= N_{\{C,G,H\}} P_{\{C,G,H\}} \Delta t \\ |G_{SM}| &= N_{SM} P_{SM} \Delta t \end{aligned} \tag{5.2}$$

It follows then that the energy generated per timestep is a function of the peak energy capacity and the dispatch level as determined by the mixed integer linear program described

by Eq. (5.3).

$$\begin{aligned} G_{D\{C,G,H\}}\left(n\Delta t\right) &= \left|G_{D\{C,G,H\}}\right| d_{\{C,G,H\}}\left(n\Delta t\right) \\ G_{SM}\left(n\Delta t\right) &= \left|G_{SM}\right| d_{SM}\left(n\Delta t\right) \end{aligned} \tag{5.3}$$

Where:

$$\begin{aligned} G_{D\{C,G,H\}}, G_{SM} &\rightarrow \text{Generated Dispatchable energy (MWhr)} \\ N_{\{C,G,H,SM\}} &\rightarrow \text{Total number of units} \\ P_{\{C,G,H,SM\}} &\rightarrow \text{Peak Power output (MW)} \\ d_{\{C,G,H,SM\}} &\rightarrow \text{Dispatch Level} \\ \Delta t &\rightarrow \text{timestep (s)} \\ n &\rightarrow \text{index} \end{aligned}$$

B. *A load model with PEV charging system*

The load model is composed of residential, commercial, and industrial loads. The residential and commercial loads are modeled from load profiles, normalized by dividing by the maximum value, from the System Advisory Model [20]. The industrial load profile for the model was developed with normalized historical load profiles from Idaho Falls Power [21]. Each of the normalized load profiles were scaled by a user defined Peak Power Demand factor and the number of units for each type of load to allow variations of load magnitude and mix to be applied.

$$L_{\{R,C,I\}}\left(n\Delta t\right) = N_{\{R,C,I\}} P_{\{R,C,I\}} \Delta t \frac{Y_{\{R,C,I\}}\left(n\Delta t\right)}{max\left(Y_{\{R,C,I\}}\right)} \tag{5.4}$$

Where:

$$
\begin{aligned}
L_{\{R,C,I\}}\left(n\Delta t\right) &\rightarrow \text{Load Demand (MWhr)} \\
N_{\{R,C,I\}} &\rightarrow \text{Total number of units} \\
P_{\{R,C,I\}} &\rightarrow \text{Peak Power demand (MW)} \\
Y_{\{R,C,I\}} &\rightarrow \text{Data Source Value} \\
\Delta t &\rightarrow \text{timestep (s)} \\
n &\rightarrow \text{index}
\end{aligned}
$$

In addition, PEV charging systems associated with residential based slow charging systems and commercially available DC fast charging systems are included as separate controllable loads. The simulation currently assigns the charging load using uniformly distributed variables to represent the PEV charging systems. Future integration of the residential PEV slow charging model developed by Scoffield and Kunz [22] into the simulation is planned to approximate the charging cycle that predominantly contributes to the load during the evening and morning hours (6:00 PM to 6:00 AM). Since the literature review did not provide evidence that a model has been developed for DC fast chargers, a uniformly distributed variable was similarly used. Extending the statistical residential charging model to fast charging stations for the time periods that are expected to predominantly contribute to the load in the late afternoon (6:00 PM to 12:00 AM), is left to future work.

C. *The Storage Model*

Grid-level storage was integrated into the simulation in order to demonstrate the benefits of such technology when used in conjunction with intermittent renewable resources. In order to account for the energy transferred to or from the grid-level storage, the storage model was developed as a coupled sink and source system. Using this approach, the storage sink behaved as a load element while the storage source element behaved as generation with constraints limiting only one to be active at a time. Initial approaches introduced nonlinearity in the objective function which was resolved by modifying the cost structure of the storage prior to evaluation of the MILP based on the current level of charge. The storage

model was integrated into the cost function defined in Eq. (5.5) and modeled as a change in the grid storage.

$$\begin{aligned} \Delta ST &= ST_{sink} - ST_{source} \\ ST_{SOC} &= ST_{SOC} + \Delta ST \end{aligned} \tag{5.5}$$

Where ΔST is the change in state of charge of the storage element, ST_{sink} and ST_{source} are the sink and source variables for power supplied to or take from the grid, and ST_{SOC} tracks the state of charge in energy units. It is noted that this approach does not currently account for losses in the storage system.

D. *Dispatch and commitment model*

The dispatch and unit commitment model is similar in nature to the Robust Energy and Reserve Dispatch model presented in [24]. It is formulated as an optimization problem that minimizes the cost of dispatch of the local resources subject to the energy conservation, energy production levels, and physical constraints associated with resources defined in Eq. (5.6).

Objective function:

$$min\ \mathrm{C} = \sum C_{rt} W_{rt}$$

Constraints: (5.6)

$$\sum W_g = \sum W_l$$

$$0 \leq P_{da} + P_{rt} \leq P_{max}$$

Where:

$C \rightarrow$ Dispatch cost

$C_{rt} \rightarrow$ Price per MWhr for real time dispatch

$W_{rt} \rightarrow$ Energy produced through real time dispatch

$W_g \rightarrow$ Total energy generated

$W_l \rightarrow$ Total energy requirement of load

$P_{da} \rightarrow$ Power allocated by day ahead dispatch

$P_{rt} \rightarrow$ Power allocated by real time dispatch

$P_{max} \rightarrow$ Maximum power available from resource

This approach was extended such that the initial formulation of the objective function accounted for the cost of energy purchased on the spot market, the cost of generation and the cost of load shedding. The formulation was later extended to include grid level storage. In order to account for costs associated with ramping the local dispatchable generation, the ramping costs were determined using the change in dispatch level from the previous timestep and was evaluated separately from the operations and fuel costs of the unit. The inclusion of the ramping term as a function of the change in dispatch level was included for clarification during the objective function formulation, and was later simplified as seen in Eq. (5.8). In addition, the load commitment flags were integrated into the objective function using Boolean negation. While these practices clarified the objective function formulation, they also resulted in a sub-optimal formulation as seen in Eq. (5.7).

Objective function:

$$min\ \mathrm{C} = \begin{cases} \sum \left[\left(C_{op} + C_f \right)_i d_i + C_j \left(d_i \left(n \right) - d_i \left(n-1 \right) \right) \right] G_i \\ + \sum \left[p_j \left(1 - d_j \right) L_j \right] + C_{SM} G_{SM} + C_{ST} \left(ST_{source} + ST_{sink} \right) \end{cases} \tag{5.7}$$

To optimize the objective function, constant terms were eliminated which resulted in the simplified objective function in Eq. (5.8). This resulted in the elimination of both the

$d_i(n-1)$ term of the ramping term as well as the negation term of the load curtailment penalty terms.

$$min\ \mathrm{C} = \begin{cases} \sum \left[\left(C_{op} + C_f + C_r \right) d_i G_i \right] - \sum \left[p_j D_j L_j \right] \\ +C_{SM} G_{SM} + C_{st} \left| \Delta ST \right| \end{cases} \tag{5.8}$$

The constraints were similarly extended to account for the ramp rate restrictions placed on the dispatchable generation sources, the storage limits, the dispatch levels all treated as continuous on the interval $[0, 1]$ and the load commitment flag as treated as discreet in the set $\{0, 1\}$. The author is aware of the simplification of a static ramping cost that should be considered as a function of the ramp rate. However, this introduces a non-linearity, which eliminates the possibility of using straightforward linear programming. For the purpose of the initial gamification with a tractable time to solve, the solution is left sub-optimal. Constraints:

$$\begin{array}{ll} \sum d_i G_i - \sum d_j L_j + d_{sm} G_{sm} = 0 & \text{Energy balance constraint} \\ \sum \left[d_i G_i \left(n \right) - d_i \left(n-1 \right) G_i \left(n-1 \right) \right] \leq \sum G_{ri} & \text{Ramp rate constraint} \\ ST_{source} - ST_{sink} + ST_{SOC} \leq max \left(ST \right) & \text{Upper storage limit} \\ ST_{source} - ST_{sink} + ST_{SOC} \geq 0 & \text{Lower storage limit} \\ d_i \in [0, 1] & \text{Generation dispatch level} \\ d_j \in \{0, 1\} & \text{Load commitment flag} \end{array} \tag{5.9}$$

The constraints above were then reformulated in terms of the decision variables which

resulted in Eq. (5.10):

$$\begin{aligned}
&\sum d_i G_i - \sum d_j L_j + d_{sm} G_{sm} = 0 && \text{Energy balance constraint} \\
&\sum d_i G_i\,(n) \leq \sum \left[G_{ri} + d_i\,(n-1)\,G_i\,(n-1)\right] && \text{Ramp rate constraint} \\
&ST_{source} - ST_{sink} \leq max\,(ST) - ST_{SOC} && \text{Upper storage limit} \\
&-ST_{source} + ST_{sink} \leq ST_{SOC} && \text{Lower storage limit} \\
&d_i \in [0, 1] && \text{Generation dispatch level} \\
&d_j \in \{0, 1\} && \text{Load commitment flag}
\end{aligned} \tag{5.10}$$

Where:

C_{op} → Operation cost of generation (USD/MWhr)

C_f → Fuel cost of generation (USD/MWhr)

C_r → Ramp up/down cost of generation (USD/MWhr)

d → Dispatch level

G → Generation capacity (MWhr

p → Penalty for load shedding (USD/MWhr

L → Load (MWhr)

The simulation was implemented in a Matlab script using the mixed-integer linear programming function, intlinprog(), to compute the minimum solution to the cost function applying the applicable constraints at each time step.

IV. Results:

To evaluate the effectiveness of the dispatch model, simulations were performed utilizing varying levels of renewable generation and PEV charging system penetration in the microgrid. Each simulation evaluated the model for 35,040 time steps which represents one year's worth of data.

Four simulations were performed which include:

- Baseline Case
  - Peak Generation Capacity: 175 MW
  - Peak Load: 140 MW
  - No Renewable Generation
  - No PEV Charging systems
- Case 2:
  - Peak Generation Capacity: 470 MW
  - Peak Load: 334.3 MW
  - No Renewable Generation
  - Peak PEV Charging Load: 9.1 MW
- Case 3:
  - Peak Generation Capacity: 410 MW
  - Peak Load: 350 MW
  - Peak Renewable Capacity: 200 MW
  - No PEV Charging systems
- Case 4:
  - Peak Generation Capacity: 410 MW
  - Peak Load: 370 MW
  - Peak Renewable Capacity: 200 MW
  - Peak PEV Charging Load: 40 MW

Table 5.1 summarizes the results of the four test cases described above.

TABLE 5.1: Summary of Test Case Feasibility

	Total Number of Non-Feasible Solutions	Feasible Solution Convergence Rate
Case 1	22	99.94%
Case 2	11	99.97%
Case 3	85	99.76%
Case 4	79	99.77%

As illustrated, the results from all four test cases show a high feasible solution convergence rate. This indicates that the linear program converged to a solution for the objective function while satisfying the constraints. The first two test cases which did not include any renewable generation produced the fewest number of infeasible solutions while the latter two cases produced the highest number of infeasible solutions. This suggested that the feasible solution convergence rate was influenced by the renewable generation penetration in

the microgrid. This was supported by observations when it was noted that the non-feasible solutions occurred during instances for which the microgrid was not importing power from the spot market contracts and was relying only on local dispatchable and renewable generation. During these instances, sudden significant decreases in load or increases in renewable generation resulted in non-feasible solutions that failed to satisfy the energy balance constraint. In both of these cases, the down ramp rate restricted the dispatchable generation from spinning down quick enough to achieve equilibrium. This resulted in instances of over-production when non-feasible solutions were encountered. The "price" of over production becomes energy that is provided to the connect transmission system without compensation, burned off as heat, or creation of a frequency instability.

V. Conclusion:

As described in Section IV, the dispatch and commitment model was generally able to determine a feasible solution. The test cases demonstrated that the model was more likely to converge to a feasible solution in the absence of renewable generation. Further, the model showed no sensitivity to increased penetration of PEV charging systems. This was observed to be the result of the limitations placed on the ramp down rate for the dispatchable generation in instances when no power is imported from spot markets. The dispatch model appears to be a feasible, albeit suboptimal, mechanism to explore time frames in a game context that will allow players to experience the effects of increased number of PEVs connected to the electricity grid. It is suggested that future work investigate the impact of curtailment of renewable resources to the feasible solution convergence rate. More optimal dispatch algorithms could be introduced given computationally tractable solutions for variable ramp rates can be implemented in future work.

5.2 Simulation Characteristics

In addition to convergence testing of the integrated dispatch algorithm as presented in Section 5.1, observations were made directly from the simulation interface, an example of which is shown in Figure 5.1.

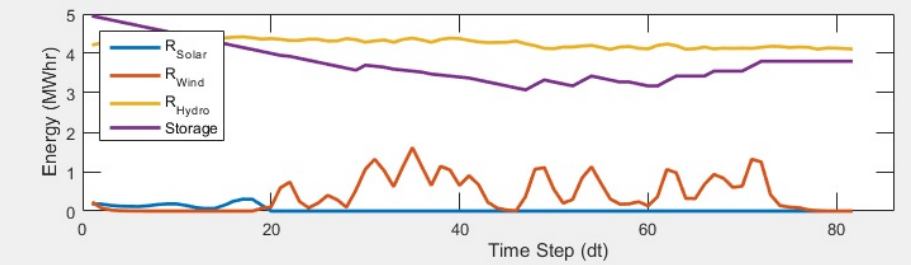

(a) Renewable Generation and Storage

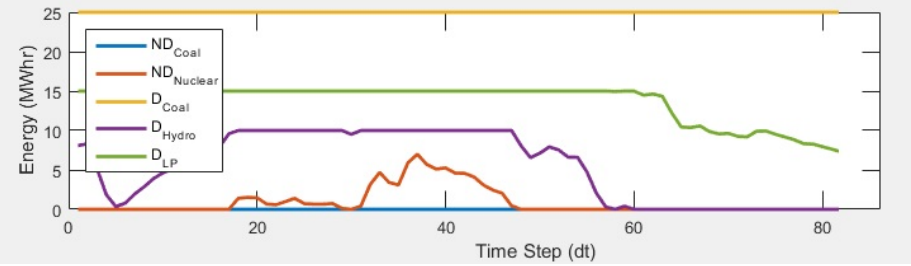

(b) Dispatchable Generation and Spot Market Contracts

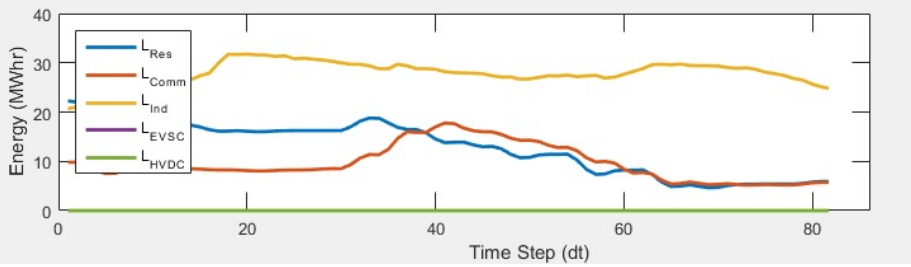

(c) Demand

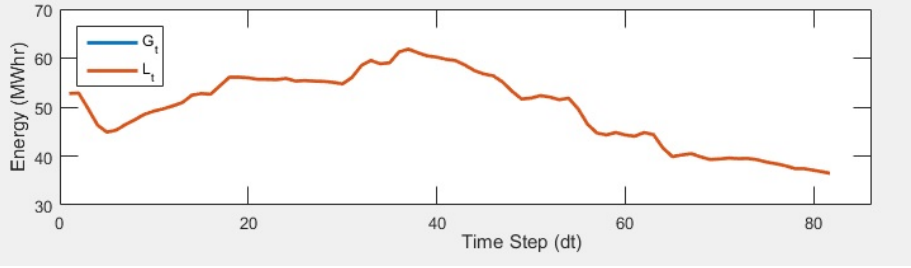

(d) Total Generation and Load

Figure 5.1: Simulation Interface Overview

As seen here, the interface is divided into four plot areas. Each plot includes the increment timestep on the horizontal axis and energy produced or consumed on the vertical axis. The plot areas were scaled to represent the previous two days of the simulation and were separated to allow the user to easily distinguish between the different types of generation and load in the system as well as to segregate elements with comparable magnitudes. In Figure 5.1, only the first 80 timesteps are illustrated to allow for adequate resolution of the data.

The upper plot area shown in Figure 5.1a represents the renewable generation and grid scale storage. This plot shows the significant variability of the wind resource compared to the limited variability of the hydroelectric resource. In addition, the plot shows on significant output from the solar resource which suggests that the data occurred during evening hours or during a period of significant cloud cover. In addition, the upper plot area shows the charge and discharge cycles of the storage element which are conditioned to prefer an average state of charge of 50% in the simulation model settings. The second plot area shown in Figure 5.1b includes the dispatchable generation, referenced in the legend as $D_{Coal}, D_{Hydro}, D_{LP}$ and the spot market energy purchases, represented as SM_{Coal} and $SM_{Nuclear}$. The energy from the spot markets were separated into these two types to allow developers to include an option to purchase energy from 'green' and 'polluting' sources. The third region shown in Figure 5.1c illustrates the load profiles for each of the load types. This particular simulation does not include load from either of the electric vehicle charging systems. Finally, in Figure 5.1d, the total load and generation are represented. Since the problem is constrained to satisfy the energy balance equation, the total generation and load will overlay each other whenever the integrated dispatch algorithm converges to a solution as shown.

5.2.1 Generation Ramp During Startup Conditions

At the beginning of the simulation, all dispatchable generation is assumed to be in an idle state. This requires the simulation to initially purchase all energy from spot markets to satisfy demand while the dispatchable generation resources to ramp up. It is expected

that the "ramp up" condition is observable during startup. Figure 5.2 shows this behavior for approximately the first 50 timesteps of the simulation. Since the dispatchable generation from coal has the slowest ramp rate of $0.05\frac{pu}{dt}$, it takes the longest to ramp to full production. Gas-fired generation has a slightly faster ramp rate of $0.1\frac{pu}{dt}$ and therefore reaches full production before dispatchable coal. Dispatchable hydroelectric has the fastest ramp rate of $0.5\frac{pu}{dt}$ and reaches full production well in advance of the thermal units.

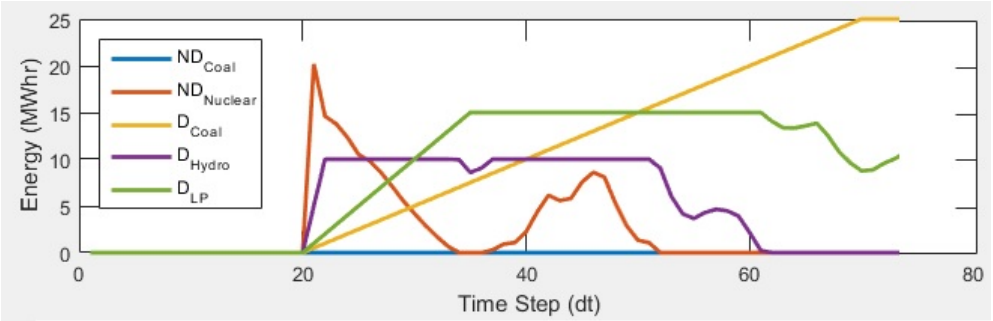

Figure 5.2: Startup Behavior of Simulation

It is noteworthy to point out that after the dispatchable units satisfy demand, the dispatchable generation with the fastest response and greatest cost is decreased while the generation with the slowest response and lowest cost is increased. Figure 5.2 additionally shows the dependency between each of the dispatchable resources and spot market contracts. As suggested, the energy purchased from spot market contracts is at the maximum during initialization and decreases as the dispatchable generation becomes available. Further, since the dispatchable generation with quick ramp rates are assigned higher costs than the resources with slower responses, the simulation prefers to ramp the slow resource to full production and decrease the dependence on the more expensive alternatives.

5.2.2 Simulation Behavior During Divergent Behavior

The results presented in Section 5.1 demonstrate the rate of convergence of the integrated dispatch algorithm during the four scenarios presented, but did not discuss the behavior of the simulation when the algorithm failed to achieve a convergent solution. Un-

der these non-convergent conditions, the simulation was developed to use the solution from the previous timestep for the current timestep. This method was developed after analysis of the simulation revealed that divergent behavior only occurred during instances when the system was operating independent of the external system. It was determined that under this condition, the integrated dispatch algorithm would fail to converge if either a sudden decrease in demand or an increase in renewable generation occurred which prevented the dispatchable generation from decreasing production quick enough to maintain the energy balance constraint. This resulted in generation exceeding demand until convergence was achieved, which generally occurred on the subsequent timestep.

Figure 5.3 shows one such non-convergent event discovered during the analysis of the third scenario described in Section 5.1. In this instance, Figure 5.3c shows a point-wise drop in the industrial load profile near timestep 52. This point-wise drop in industrial load is suspected to be the result of a recloser operation recorded in the dataset. As a result, the previous solution for the dispatchable generation was carried forward and resulted in no change in production for that timestep as seen in Figure 5.3b. This caused the generation to exceed demand for the subsequent timestep, and thereafter, the simulation converged to a solution and consequently restored energy balance in the system as seen in Figure 5.3d.

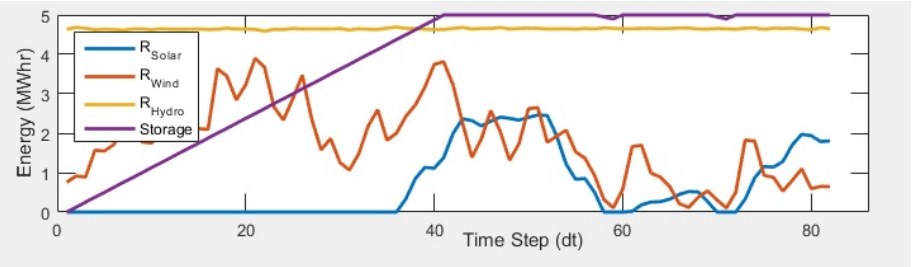

(a) Renewable Generation and Storage

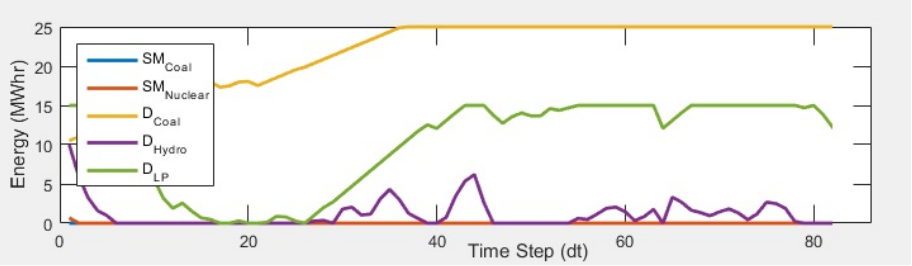

(b) Dispatchable Generation and Spot Market Contracts

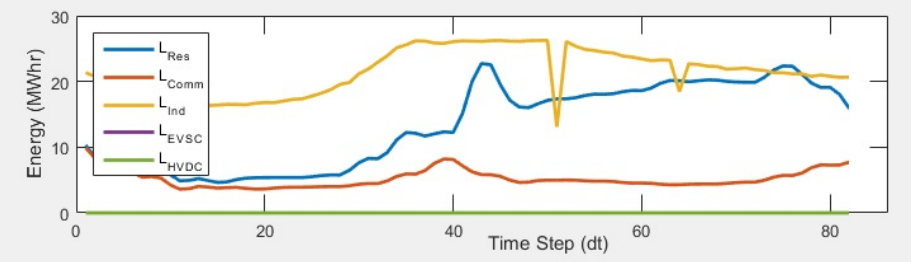

(c) Demand

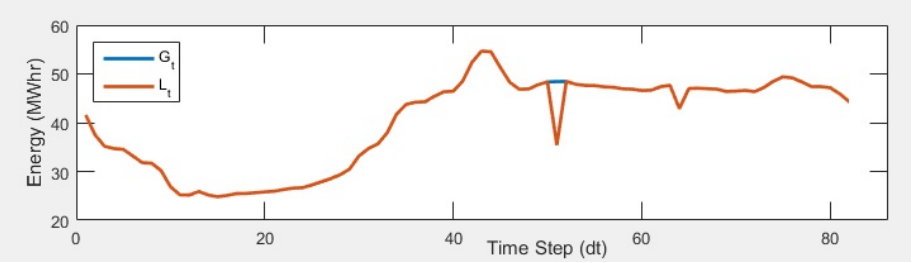

(d) Total Generation and Load

Figure 5.3: Energy Balance during Divergent Solution

Chapter 6: Summary and Future Work

6.1 Conclusion

This thesis presented the development of an integrated dispatch algorithm, which was developed to determine the optimal economic dispatch and demand response decisions given a set of inputs from generation and load elements. This algorithm is unique in that it allows both traditional generation and load elements as well as generation from renewable resources and loads from electric vehicle charging systems. The work presented a brief discussion of renewable energy resources and electric vehicle charging systems and the challenges these present for traditional economic dispatch and demand response methods. It then provided a short introduction to linear programming techniques which serve as the optimization technique used in this study as well as the economic dispatch, demand response and unit commitment problems in the context of linear programming. The thesis then presented the integrated dispatch algorithm, which combined these three problems and described the definition of the inputs representing the generation and load types used for testing and evaluation.

The subsequent development of the simulation in MatLab allowed for testing of the algorithm under various conditions. These results showed that under a variety of test conditions, the algorithm converged in excess of 99.97% of the time. Additionally, the behavior of the system during startup and under periodic variations was demonstrated.

6.2 Future Work

In evaluating the project, several key aspects were highlighted that provide opportunities for future development of this work.

These opportunities for the future development of this work include.

1. Revise the integrated dispatch algorithm such that the decision variables for the generation units represent the change in level of generation rather than the dispatch level.
2. Implement inputs as discrete generation sources and loads rather than aggregate elements.
3. Include provisions to allow for critical non-curtailable loads to represent critical infrastructure such as hospitals and emergency response centers.
4. Implement a model such as that presented by Scoffield [22] for the residential based electric vehicle charging systems.
5. Develop or identify a model for commercial based electric vehicle charging systems, in particular direct current fast chargers.

In the current implementation, the generation and load levels are evaluated in the objective function to determine the optimal dispatch of generation and curtailment of load to satisfy the energy balance equation. In reflection, this is unnecessary as suggested above. In fact, only the change in generation or load level needs to be evaluated in the objective function, similar to the manner that the energy storage was evaluated. This was observed late in the project and therefore it was not feasible to revise the implementation. In the second case, the scope of the project limited the development to aggregate models of the generation and load elements. This provided a simplified approach that was transferable to other programming environments, but included only a few representative elements. As an alternative, non-aggregated inputs could be developed to provide multiple models for the different types of loads and generation resources. This would also allow for the inclusion of critical loads such as those suggested above.

In addition to these opportunities for improvement, this project also identified that established models for electric vehicle charging systems are still in the developmental stages. While effort has been exerted to develop models for residential charging systems, no such models were identified for commercially installed charging systems such as the high voltage direct current systems. Because of this, significant opportunity exists to develop these models as data becomes available.

References

[1] M. R. Jabłońska, "Renewable Energy System Management Processes in Smart Grid Operation," in *Economy and Management*, pp. 121-130, 2012.

[2] R. C. Green II, L. Wang, M. Alam, "The impact of plug-in hybrid electric vehicles on distribution networks: A review and outlook," in *Renewable and Sustainable Energy Reviews*, vol. 15, pp. 544-553, 2011.

[3] "Electric Vehicle Market Penetration: An examination of industry literature," in *Issues in brief*, The Texas Transportation Institute, Strategic Solutions Center, # 2011-01, 2011.

[4] T. B. Christensen, T. E. Lorentzen, T. Bertelsen, S. Lũck, R. Marrbjeg, *Establishing the investment case: Wind power,* Deloitte Touche Tohmatsu Limited, April 2014.

[5] Edison Technology Center, (2016, Sept. 29), *History of Electric Cars,* [Online]. Available: http://edisontechcenter.org/ElectricCars.html.

[6] U.S. Department of Energy, Office of Energy Efficiency and Renewable Energy, (2016, Sept. 29) *History of Hydropower,* [Online]. Available: http://energy.gov/eere/water/history-hydropower.

[7] L. Dickerman and J. Harrison, "A New Car, a New Grid," in *IEEE Power and Energy Magazine*, vol. 8, no. 2, pp. 55-61, March-April 2010. doi: 10.1109/MPE.2009.935553

[8] U.S Energy Information Administration, "Short-Term Energy Outlook," Analysis and Projections, August 2016.

[9] C. Tseng, S. S. Oren, C. S. Cheng, C. Li, A. J. Svoboda, R. B. Johnson, "A transmission-constrained unit commitment method in power system scheduling," in *Decision Support Systems*, 24(3-4), 297-310. 1998 doi:10.1016/s0167-9236(98)00072-4

[10] J. P. Fossati, "Unit Commitment and Economic Dispatch in Micro Grids", in *Memoria de Trabajos de Difusión Científica y Técnica*, núm. 10, September 2012.

[11] T. McJunkin, C. Rieger, B. Johnson, D. S. Naidu, L. Beaty, J. Gardner, I. Ray, K. L. Blanc, M. Guryan, "Interdisciplinary Education through Edu-tainment: Electric Grid Resilient Control Systems Course," in *2015 ASEE Annual Conference and Exposition Proceedings*, 2015.

[12] "The Potential Benefits of Distributed Generation and the Rate-Related Issues That May Impede Its Expansion," Report Pursuant to Section 1817 of the Energy Policy Act of 2005, United States Department of Energy, 2005.

[13] US Department of Energy, (10 Sept. 2016), *Microgrid Definitions,* [Online], Available: https://building-microgrid.lbl.gov/microgrid-definitions

[14] M. Shahidehpour, H. Yamin, Z. Li, "Security Constrained Unit Commitment," in *Market Operations in Electric Power Systems: Forecasting, Scheduling, and Risk Management*, 1, Wiley-IEEE Press, 2002, pp.275-310 doi: 10.1002/047122412X.ch8

[15] *Energy Policy Act of 2005*. Pub.L 109-58, Washington, D.C.: U.S. G.P.O.

[16] L. A. Wolsey, G. L. Nemhauser, "I.2: Linear Programming" in *Wiley Series in Discrete Mathematics and Optimization: Integer and Combinatorial Optimization*, Wiley-Interscience, 1999, ch. I.2 ,pp. 27-49

[17] Jizhong Zhu, "Classic Economic Dispatch," Optimization of Power System Operation, Wiley-IEEE Press, 2015, pp.84-140 doi: 10.1002/9781118887004.ch4

[18] National Solar Radiation Database, Renewable Resource Data Center, National Renewable Energy Laboratory, US Department of Energy, (19 Aug. 2016), "Solar Resource Information", [Online], Available: http://rredc.nrel.gov/solar/old_data/nsrdb/

[19] Vestas Corporation, (2016), "V110 2.0 MWTM at a Glance", [Online], Available: http://www.vestas.com/en/products/turbines/v1102_0_mw#!power curveandaep

[20] National Renewable Energy Laboratory, (30 Jul. 2016), "Welcome to SAM", System Advisory Model (SAM), [Online], Available: http://sam.nrel.gov

[21] Center for Advanced Energy Studies-Wind for Schools, (15 Oct. 2016), "Idaho Falls Power Hydro Energy Production and Load", [Online], Available: http://wind-for-schools.caesenergy.org/wind-for-schools/IF_ Power.html

[22] D. Scoffield, M. R. Kunz, "Impact of plug-in electric vehicle charge rates on residential demand", in *IEEE Conference on Technologies for Sustainability 2015*, Ogden, Utah, August 2015.

[23] W. Wei, F. Liu, S. Mei and Y. Hou, "Robust Energy and Reserve Dispatch Under Variable Renewable Generation," in *IEEE Transactions on Smart Grid*, vol. 6, no. 1, pp. 369-380, Jan. 2015. doi: 10.1109/TSG.2014.2317744B.

[24] B. Zhang, R. Rajagopal and D. Tse, "Network Risk Limiting Dispatch: Optimal Control and Price of Uncertainty," in *IEEE Transactions on Automatic Control*, vol. 59, no. 9, pp. 2442-2456, Sept. 2014.

Appendix A: Matlab Code for Simulation

The following MATLAB code represents the simulation developed to test the integrated dispatch model.

```
function MedTimeSimV5(Ng, Nl)
%
% Description:
%       Function to test solution convergence and feasibility for mixed
%       integer linear program model developed for 15 minute unit commitment
%       and dispatch
% Input:
%       Ng -> Number of generators
%                [Sol_R, Wind_R, Hydro_R, Coal_ND, Nuclear_ND,
%                 Coal_D, Hydro_D, LP_D, Storage]
%      Nl -> Number of load elements
%                [Res, Comm, Ind, DR, EVSC, DCFC]
% Test Case 1:
%       MedTimeSimV5([0,0,0,1,1,1,1,1],[4,2,1,0,0,0])
%       175 MW capacity, 140 MW load, no renewable generation/PEV
%       penetration, No storage
%       Non-Feasable Solutions:  22  (0.063%%)
% Test Case 2:
%       MedTimeSimV5([0,0,0,4,2,2,4,3],[10,5,2,0,800,150])
%       470 MW peak capacity, 334.3 MW peak load, No Renewable/
%                                                 High PEV penetration,
%       No storage
%       Non-Feasable Solutions:  11 (0.0314%)
% Test Case 3:
%       MedTimeSimV5([20,10,2,2,2,2,2,2],[10,4,3,0,0,0])
%       410 MW capacity, 350 MW load, high renewable/PEV penetration,
%       Non-Feasable Solutions:
% Test Case 4:
%       MedTimeSimV5([20,10,2,2,2,2,2,2],[10,4,2,0,10000,1000])
%       410 MW capacity, 350 MW load, high renewable/PEV penetration,
%       Non-Feasable Solutions:
% ================================================================
%Time step definition
    dt = 0.25;  %1/4 hour timestep
%Accumulated Revenue initial condition
    Acc_Net_Income = 1e6;
% Initializes parameter sets
    [Gen_Data,Load_Data,Storage_Data,Line_Data]=InitializeDataStructures();
% Import Raw and Normalized data from external sources
```

```
    FifteenMinuteData=ImportData(dt);
%==========================================================================
% Update number of units from Ng and Nl input vectors
Gen_Data(1:8,1)=Ng';
Load_Data(1:6,1)=Nl';
%==========================================================================
% Start Simulation
StartSimulation(dt, Gen_Data, Storage_Data, Load_Data,...
                Line_Data, FifteenMinuteData);
end

function StartSimulation(dt, Gen_Data, Storage_Data,...
                         Load_Data, Line_Data, FifteenMinuteData)
%Pricing data sources:
    %       https://en.wikipedia.org/wiki/Cost_of_electricity_by_source
    %       http://www.nei.org/CorporateSite/media/filefolder/Policy/
    %           Papers/Nuclear-Costs-in-Context.pdf?ext=.pdf

    %       Customer Cost will be $115/MWhr from average Residential
    %       Utility Rate for Idaho

    %Weekly Load/Gen history
    %Row Definition:
        %1  -> Solar (MWhr)
        %2  -> Wind (MWhr)
        %3  -> Hydro-ROR (MWhr)
        %4  -> ND_Coal (MWhr)
        %5  -> ND_Nuclear (MWhr
        %6  -> D_Coal (MWhr)
        %7  -> D_Hydro (MWhr)
        %8  -> D_Natural Gas (MWhr)
        %9  -> Residential (MWhr)
        %10 -> Commercial (MWhr)
        %11 -> Industrial (MWhr)
        %12 -> EV Slow charge (MWhr)
        %13 -> EV Fast charge (MWhr)
        %14 -> System Faults (MWhr)
        %15 -> Total Generation (MWhr)
        %16 -> Total Load (MWhr)
        %17 -> Storage (MWhr)
        %18 -> Solar - Storage
        %19 -> Wind - Storage
        %20 -> Hydro-ROR - Storage
    Daily_Data = zeros(20,192);
%==========================================================================
    index = 1;
    [DatRow, DatCol] = size(FifteenMinuteData);
```

```
    plotwidth = 192;
    IndVar = 1:plotwidth;
    count=0
    while(index<=DatCol)  %upper limit generally set to DatCol
        Daily_Data(:,1:plotwidth-1)=Daily_Data(:,2:plotwidth);
%=========================================================================
    % Renewable Generation
        %Solar Data for current Timestep
        Gen_Data(1,9)=dt*Gen_Data(1,1)*Gen_Data(1,3)*...
                      FifteenMinuteData(1,index);
       %Wind Data for current Timestep
        Gen_Data(2,9)=dt*Gen_Data(2,1)*Gen_Data(2,3)*...
                      FifteenMinuteData(2,index);
        %Hydro Data for current Timestep
        Gen_Data(3,9)=dt*Gen_Data(3,1)*Gen_Data(3,3)*...
                      FifteenMinuteData(3,index);
    %=========================================================================
    % Load Profiles
        %Residential Load Data
        Load_Data(1,7)=dt*Load_Data(1,1)*Load_Data(1,3)*...
                       FifteenMinuteData(4,index);
        %Commercial Load Data
        Load_Data(2,7)=dt*Load_Data(2,1)*Load_Data(2,3)*...
                       FifteenMinuteData(5,index);
        %Industrial Load Data
        Load_Data(3,7)=dt*Load_Data(3,1)*Load_Data(3,3)*...
                       FifteenMinuteData(6,index);
        %PEV Slow Charge Data
            %Randomly calculated to stress model
        Load_Data(5,7)=dt*Load_Data(5,1)*Load_Data(5,3)*(0.3+0.7*rand(1));
        %PEV Fast Charge Data
            %Randomly calculated to stress model
        Load_Data(6,7)=dt*Load_Data(6,1)*Load_Data(6,3)*(0.2+0.8*rand(1));
%=========================================================================
    % Determine optimal generation dispatch level and load commitment based
    % on constraints and cost function
        Storage_Data=CostOfStorage(Storage_Data,Gen_Data,dt);
        [result, fval, flag] = MILP(dt, Gen_Data, Load_Data,...
                                    Storage_Data, Line_Data);
        if flag~=1
            count=count+1
        end
        count
%=========================================================================
    if(~isempty(result))
    %Record Dispatch/Commit decision
        Gen_Data(4:8,10)=result(1:5);
```

```
        Load_Data(1:3,8)=result(6:8);
        Load_Data(5:6,8)=result(9:10);
        Storage_Data(1:2,8) = result(11:12);
    %Record Instantaneous Value
        Gen_Data(4:5,9)=dt*Gen_Data(4:5,1).*...
                        Gen_Data(4:5,3).*Gen_Data(4:5,10);
        Gen_Data(6:8,9)=dt*Gen_Data(6:8,1).*...
                        Gen_Data(6:8,3).*Gen_Data(6:8,10);
        Load_Data(1:3,7)=Load_Data(1:3,8).*Load_Data(1:3,7);
        Load_Data(5:6,7)=Load_Data(5:6,8).*Load_Data(5:6,7);
        Storage_Data(1,7)=dt*Storage_Data(1,1).*...
                          Storage_Data(1,4).*result(11);
        Storage_Data(2,7)=dt*Storage_Data(2,1).*...
                          Storage_Data(2,4).*result(12);
        Storage_Data(3,7)=Storage_Data(3,7)-...
                          Storage_Data(1,7)+...
                          Storage_Data(2,7);
    end
%=========================================================================
      % Determine Cost of Storage and charge rate from current
    % state of charge
    % Update Daily Data
        Daily_Data(1:8,plotwidth)=Gen_Data(1:8,9);
        Daily_Data(9:13,plotwidth)=[Load_Data(1:3,7);Load_Data(5:6,7)];
        Daily_Data(15:17,plotwidth)=[sum(Gen_Data(1:3,9))+...
                                     (1-Line_Data(1,2))*sum(Gen_Data(4:5,9))+...
                                     sum(Gen_Data(6:8,9))+Storage_Data(1,7)-...
                                     Storage_Data(2,7);
                                     sum(Load_Data(1:6,7));
                                     Storage_Data(3,7)];
%=========================================================================
      Update_Plot(IndVar,Daily_Data);
        index=index+1;
    end
    assignin('base','Gen_Data',Gen_Data);
    assignin('base','Load_Data',Load_Data);
    assignin('base','Storage_Data',Storage_Data);
    assignin('base','Daily_Data',Daily_Data);
    assignin('base','dt',dt);
end

function [Gen_Data, Load_Data, Storage_Data,...
          Line_Data]=InitializeDataStructures()
%Generation Data
    %Row Definition:
        %1 -> Solar (Renewable, Non-Dispatchable)
        %2 -> Wind (Renewable, Non-Dispatchable)
```

```
        %3 -> Hydro (Run of River, Non-Dispatchable)
        %4 -> Spot Market Coal (Non-Dispatchable)
        %5 -> Spot Market Nuclear (Non-Dispatchable)
        %6 -> Local Coal (Dispatchable)
        %7 -> Hydro (Spinning Reserve, Dispatchable)
        %8 -> Natural Gas (Flat Start capable, Dispatchable)

%Column Definition:
        %1 -> Current # Units
        %2 -> Max # Units
        %3 -> Power/Unit (MW)
        %4 -> Ramp up rate (MW/dt)
        %5 -> Ramp down rate (MW/dt)
        %6 -> Fuel Cost (USD/MWhr)
            %http://www.eia.gov/coal/markets/
                %Average cost per ton of coal: $35/ton
            %http://www.nei.org/Master-Document-Folder/Backgrounders/
            %       White-Papers/Nuclear-Costs-in-Context
                %Average nuclear fuel cost per MWhr: $7/MWhr
        %7 -> Ramp up costs (USD/???)
        %8 -> Operation cost (USD/MWhr)
            %http://www.nei.org/Master-Document-Folder/Backgrounders/
            %       White-Papers/Nuclear-Costs-in-Context
                %Average Operating Cost per MWhr: $35/MWhr
        %9 -> Instantaneous Value
        %10-> Percent Dispatched

        %Pricing is set artificially and will need to be refined.
Gen_Data = [0,  10,   1,   0,    0,    0,    0, 115,  0,  1;
            0,  20,   2,   0,    0,    0,    0, 105,  0,  1;
            0,   1,  10,   0,    0,    0,    0,  95,  0,  1;
            0,  10,  25,   0,    0,   90,    0,  35,  0,  1;
            0,   5,  50,   0,    0,   35,    0,  80,  0,  1;
            0,  10,  50,  10,    1,   80,   50,  10,  0,  0;
            0,   5,  20,  20,   10,    0,   10,  75,  0,  0;
            0,   5,  30,  10,    2,   60,   30,  25,  0,  0];
%Storage Data
    %Row definition:
        %1 -> Storage Source (acts like generation)
        %2 -> Storage Sink (acts like load)
        %3 -> State of charge (Preserves charge state)
                % Only Instantaneous value is used.
    %Column definition
        %1 -> Current # Units
        %2 -> Max # Units
        %3 -> Storage Capacity/Unit (MW)
        %4 -> Charge/Discharge rate (MW/dt)
```

```
        %5 -> Charge/Discharge costs (USD/MWhr)
        %6 -> Operation cost (USD/MWhr)
        %7 -> Instantaneous Value
        %8 -> change in charge/Percent charged (row 3)
% Storage values are initialized assuming no initial charge
Storage_Data = [10, 20, 2, 0.001, 100, 10, 0, 0;
                10, 20, 2, 0.010,  10, 10, 0, 0;
                10, 20, 2,     0,   0,  0, 0, 0];
%Load Data
    %Row Definition:
        %1 -> Residential (high rate, low shed preference)
        %2 -> Commercial (medium rate, medium shed preference)
        %3 -> Industrial (medium rate, low shed preference)
        %4 -> Demand Response (low rate, high shed preference)
        %5 -> EV Slow charge (low rate, high shed preference)
        %6 -> EV Fast charge (low rate, high shed preference)
        %7 -> System Faults (no rate, no shed preference, high burden)
    %Column Definition:
        %1 -> Current # zones
        %2 -> Max # zones
        %3 -> Peak Power demand/zone (MW)
        %4 -> Energy cost (USD/MWhr)
        %5 -> Penalty cost for curtailment (USD/MWhr)
        %6 -> Load Shed Preference (serves as weighting coefficient)
            %0 = no load shedding capable
            %1 = low
            %2 = medium
            %3 = high
        %7 -> Instantaneous Value
        %8 -> Unit Commit Flag
   Load_Data = [1,      25,     10,  120,  360,  1,   0,   1;
                1,      25,     25,  110,  330,  2,   0,   1;
                0,      10,     50,  105,  315,  2,   0,   1;
                0,      10,     10,  100,  300,  3,   0,   1;
                0,  100000,   2e-3,   95,  285,  3,   0,   1;
                0,    1000,  50e-3,   95,  285,  3,   0,   1;
                0,       1,    250,    0,    0,  0,   0,   1];
%Line Data
        %Only external contracts incur transmission costs and are subject
        %to line limits.  Specifically, Spot market contracts and in the
        %future day ahead contracts and player contracts will be subject to
        %these restrictions.
    %Row Definition:
        %1 -> Transmission line data

    %Column Definition:
        %1 -> Transmission Cost (USD/MWhr)
```

```
        %2 -> Line loss (Percent of total energy transmission)
        %3 -> Line limit (MW)
    Line_Data = [5, 0.02, 200];
end

function FifteenMinuteData=ImportData(dt)
%=========================================================================
%Raw Data from external sources

    %Row         Description
    %  1            Normalized Solar Radiation
    %  2            Raw Wind Speed (MPH)
    %  3            Normalized RoR Hydro
    %  4            Normalized Residential Load
    %  5            Normalized Commercial Load
    %  6            Normalized Industrial
if(~exist('C:\Users\DAVING\Documents\FifteenMinuteData.xlsx','file'))
    FifteenMinuteData = zeros(6,8760/dt);

    %=============================================
    % Read Solar Radiation Data from NREL repository
        URL = strcat('http://rredc.nrel.gov/solar/old_data/',...
                     'nsrdb/1991-2010/data/hourly/725785/',...
                     '725785_2010_solar.csv');
        options=weboptions('Timeout',60);
        websoldata = webread(URL,options);
        soldata = websoldata.METSTATDir_Wh_m_2_;

    %=============================================
    % Read Residential and Commercial Load profile from NREL SAM model
    % Data from NREL System Advisor Model (SAM)
    % https://www.nrel.gov/analysis/sam/help/html-php/
    %       index.html?electric_load.htm
    NREL_Data=xlsread('NREL_ResComm_8760_Data.xlsx');
    comdata=NREL_Data(:,1);
    resdata=NREL_Data(:,2);
        %Extract Measured Direct Normal Solar Radiation from data
        %source
        [NREL_Row,NREL_Col] = size(NREL_Data);
        %Interpolate raw solar data for 15 minute data
        index = 1;
        for i=1:NREL_Row/dt
            if index<8760
            %Raw Solar
            FifteenMinuteData(1,i)=((mod(i,4)+1)/4)*(soldata(index+1)-...
                        soldata(index))+soldata(index+1);
            %Raw Residential
```

```
        FifteenMinuteData(4,i)=((mod(i,4)+1)/4)*(resdata(index+1)-...
                        resdata(index))+resdata(index+1);
        %Raw Commercial
        FifteenMinuteData(5,i)=((mod(i,4)+1)/4)*(comdata(index+1)-...
                        comdata(index))+comdata(index+1);
        else
            FifteenMinuteData(1,i)=soldata(index);
            FifteenMinuteData(4,i)=resdata(index);
            FifteenMinuteData(5,i)=comdata(index);
        end
        if(mod(i,4)==0)
            index=index+1;
        end
    end

%Read Windspeed, Hydro Gen, Load data from Idaho Falls Data
%from CAES website:
%http://wind-for-schools.caesenergy.org/phphydrodata.php?num=10000
    CAES_Data = xlsread('IFPSolarHydroDataCorrected.xlsx');
    [CAES_Row, ~] = size(CAES_Data);
    index = 1;
    for i=1:CAES_Row
        switch(mod(i-1,6))
            case {0, 3}      %Top/Half past the Hour Raw Data
                FifteenMinuteData(2,index) = CAES_Data(i,9);
                                                %Wind Speed
                FifteenMinuteData(3,index) = CAES_Data(i,3);
                                                %Average Raw of
                                                %ROR hydro Data
                FifteenMinuteData(6,index) = CAES_Data(i,5);
                                                %Raw Load Data
                index=index+1;
            case 1      %15 past/to the hour Raw Data
                FifteenMinuteData(2,index) = (CAES_Data(i,9)+...
                                              CAES_Data(i+1,9))/2;
                                                %Wind Speed
                FifteenMinuteData(3,index) = (CAES_Data(i,3)+...
                                              CAES_Data(i+1,3))/2;
                                                %Average Raw of
                                                %ROR hydro Data
                FifteenMinuteData(6,index) = (CAES_Data(i,5)+...
                                              CAES_Data(i+1,5))/2;
                                                %Raw Load Data
                index=index+1;
            case 5      %15 past/to the hour Raw Data
                FifteenMinuteData(2,index) = (CAES_Data(i-1,9)+...
                                              CAES_Data(i,9))/2;
```

```
                                                    %Wind Speed
                    FifteenMinuteData(3,index) = (CAES_Data(i-1,3)+...
                                                  CAES_Data(i,3))/2;
                                                    %Average Raw of
                                                    %ROR hydro Data
                    FifteenMinuteData(6,index) = (CAES_Data(i-1,5)+...
                                                  CAES_Data(i,5))/2;
                                                    %Raw Load Data
                    index=index+1;
                end
            end
            % Normalize Solar data
            FifteenMinuteData(1,:)=FifteenMinuteData(1,:)/...
                                   max(FifteenMinuteData(1,:));
            % Normalized for 2MW, Vesta V110 Power Curve Characteristics
            %http://www.vestas.com/en/products/turbines/
            %       v110-2_0_mw#!power-curve-and-aep
            FifteenMinuteData(2,:)=(((2.5*FifteenMinuteData(2,:)-3)/9).*...
                                    ((2.5*FifteenMinuteData(2,:)>=3)-...
                                     (2.5*FifteenMinuteData(2,:)>=12))+...
                                    ((2.5*FifteenMinuteData(2,:)>=12)-...
                                     (2.5*FifteenMinuteData(2,:)>=20)));
            % Normalize ROR Hydro data
            FifteenMinuteData(3,:)=FifteenMinuteData(3,:)/...
                                   max(FifteenMinuteData(3,:));
            % Normalize Industrial data
            FifteenMinuteData(6,:)=FifteenMinuteData(6,:)/...
                                   max(FifteenMinuteData(6,:));
        % Average data for smoothing
        for i=2:NREL_Row/dt-1
            FifteenMinuteData(1,i)=sum(FifteenMinuteData(1,i-1:i+1))/3;
            if(FifteenMinuteData(1,i)<0)
                FifteenMinuteData(1,i)=0;
            end
            FifteenMinuteData(2,i)=sum(FifteenMinuteData(2,i-1:i+1))/3;
            FifteenMinuteData(4,i)=sum(FifteenMinuteData(4,i-1:i+1))/3;
            FifteenMinuteData(5,i)=sum(FifteenMinuteData(5,i-1:i+1))/3;
        end
        assignin('base','FifteenMinuteData',FifteenMinuteData);
        xlswrite('FifteenMinuteData.xlsx',...
                 FifteenMinuteData');
else
    FifteenMinuteData=xlsread('FifteenMinuteData.xlsx')';
    assignin('base','FifteenMinuteData',FifteenMinuteData);
end

end
```

```
function Storage_Data=CostOfStorage(Storage_Data,Gen_Data,dt)
    % This iteration associates storage with renewable generation
    % A similar structure can be used to associate storage with hour ahead
    % predictions
    if(Gen_Data(1,9)+Gen_Data(2,9)+Gen_Data(3,9)>=...
            dt*Storage_Data(3,1)*Storage_Data(3,3))
        %=================================================================
        % Cost of energy storage - High Renewable Generation
            Storage_Data(1:2,4) = [0.01;0.05];   % Discharge/Charge rates
            Storage_Data(1:2,5) = [100;-120];    % Discharge/Charge costs
    elseif(Gen_Data(1,9)+Gen_Data(2,9)+Gen_Data(3,9)<...
            1e-4*dt*Storage_Data(3,1)*Storage_Data(3,3))
        %=================================================================
        % Cost of energy storage - High Renewable Generation
            Storage_Data(1:2,4) = [0.05;0.01];   % Discharge/Charge rates
            Storage_Data(1:2,5) = [-120;100];    % Discharge/Charge costs
    else
        %=================================================================
        % Cost of energy storage - Nominal case
        if(Storage_Data(3,7)<0.10*Storage_Data(3,1)*Storage_Data(3,3))
            Storage_Data(1:2,4) = [0.01;0.05];   % Discharge/Charge rates
            Storage_Data(1:2,5) = [100;-100];    % Discharge/Charge costs
        elseif(Storage_Data(3,7)<0.35*Storage_Data(3,1)*Storage_Data(3,3))
            Storage_Data(1:2,4) = [0.02;0.04];  % Discharge/Charge rates
            Storage_Data(1:2,5) = [50;-50];      % Discharge/Charge costs
        elseif(Storage_Data(3,7)<0.65*Storage_Data(3,1)*Storage_Data(3,3))
            Storage_Data(1:2,4) = [0.03;0.03]; % Discharge/Charge rates
            Storage_Data(1:2,5) = [0;0];         % Discharge/Charge costs
        elseif(Storage_Data(3,7)<0.80*Storage_Data(3,1)*Storage_Data(3,3))
            Storage_Data(1:2,4) = [0.04;0.02];  % Discharge/Charge rates
            Storage_Data(1:2,5) = [-50;50];      % Discharge/Charge costs
        else
            Storage_Data(1:2,4) = [0.05;0.01]; % Discharge/Charge rates
            Storage_Data(1:2,5) = [-100;100];  % Discharge/Charge costs
        end
    end
end

function [result, fval, flag]=MILP(dt, Gen_Data,...
                                   Load_Data, Storage_Data, Line_Data)

% Decision variables represent % of full capacity of resource
% In case of Generation and storage, these are continuous on the interval
% [0,1]
% In the case of load, these are discrete and are elements of {0,1}
% MILP for UC/UD
```

```
%f Definition
%   Line 1-2:  Spot Market - Coal
%   Line 3-4:  Spot Market - Nuclear
%   Line 5:    Dispatchable Coal
%   Line 6:    Dispatchable Hydro
%   Line 7:    Dispatchable Gas
%   Line 8:    Residential Load
%   Line 9:    Commercial Load
%   Line 10:   Industrial Load
%   Line 11:   PEV Slow Charge
%   Line 12:   PEF Fast Charge DCFC
%   Line 13:   Storage Source (Generation)
%   Line 14:   Storage Sink (Load)
f = [(1-Line_Data(1,2))*(Gen_Cost(Gen_Data(4,6:8))+...
      Line_Data(1,1))*dt*Gen_Data(4,1)*Gen_Data(4,3);
     (1-Line_Data(1,2))*(Gen_Cost(Gen_Data(5,6:8))+...
      Line_Data(1,1))*dt*Gen_Data(5,1)*Gen_Data(5,3);
     Gen_Cost(Gen_Data(6,6:8))*dt*Gen_Data(6,1)*Gen_Data(6,3);
     Gen_Cost(Gen_Data(7,6:8))*dt*Gen_Data(7,1)*Gen_Data(7,3);
     Gen_Cost(Gen_Data(8,6:8))*dt*Gen_Data(8,1)*Gen_Data(8,3);
     -Load_Data(1,7)*Load_Data(1,5);
     -Load_Data(2,7)*Load_Data(2,5);
     -Load_Data(3,7)*Load_Data(3,5);
     -Load_Data(5,7)*Load_Data(5,5);
     -Load_Data(6,7)*Load_Data(6,5);
     sum(Storage_Data(1,5:6))*dt*Storage_Data(1,1)*Storage_Data(1,4);
     sum(Storage_Data(2,5:6))*dt*Storage_Data(2,1)*Storage_Data(2,4)];

intcon = [6,7,8,9,10];

A = [(1-Line_Data(1,2))*dt*Gen_Data(4,1)*Gen_Data(4,3),...
     (1-Line_Data(1,2))*dt*Gen_Data(5,1)*Gen_Data(5,3),...
                                          0, 0, 0, 0, 0, 0, 0, 0, 0, 0;
     0, 0, dt*Gen_Data(6,1)*Gen_Data(6,3),  0, 0, 0, 0, 0, 0, 0, 0, 0;
     0, 0, 0,  dt*Gen_Data(7,1)*Gen_Data(7,3), 0, 0, 0, 0, 0, 0, 0, 0;
     0, 0, 0, 0,  dt*Gen_Data(8,1)*Gen_Data(8,3), 0, 0, 0, 0, 0, 0, 0;
     0, 0, -dt*Gen_Data(6,1)*Gen_Data(6,3), 0, 0, 0, 0, 0, 0, 0, 0, 0;
     0, 0, 0, -dt*Gen_Data(7,1)*Gen_Data(7,3), 0, 0, 0, 0, 0, 0, 0, 0;
     0, 0, 0, 0, -dt*Gen_Data(8,1)*Gen_Data(8,3), 0, 0, 0, 0, 0, 0, 0;
     0, 0, 0, 0, 0, 0, 0, 0, 0, 0,...
     -dt*Storage_Data(1,1)*Storage_Data(1,4),...
     dt*Storage_Data(2,1)*Storage_Data(2,4);
     0, 0, 0, 0, 0, 0, 0, 0, 0, 0,...
     dt*Storage_Data(1,1)*Storage_Data(1,4),...
     -dt*Storage_Data(2,1)*Storage_Data(2,4)];
 % b Definition:
 %   Line 1:    Line limit
```

```
    %   Line 2-4:  Gen Ramp Up Constraint
    %   Line 5-7:  Gen Ramp Down Constraint
    %   Line 8:    Storage Upper Limit
    %   Line 9:    Storage Lower Limit
    b =[dt*Line_Data(1,3);
        dt*Gen_Data(6,1)*(Gen_Data(6,5)+Gen_Data(6,10)*Gen_Data(6,3));
        dt*Gen_Data(7,1)*(Gen_Data(7,5)+Gen_Data(7,10)*Gen_Data(7,3));
        dt*Gen_Data(8,1)*(Gen_Data(8,5)+Gen_Data(8,10)*Gen_Data(8,3));
        dt*Gen_Data(6,1)*(Gen_Data(6,4)-Gen_Data(6,10)*Gen_Data(6,3));
        dt*Gen_Data(7,1)*(Gen_Data(7,4)-Gen_Data(7,10)*Gen_Data(7,3));
        dt*Gen_Data(8,1)*(Gen_Data(8,4)-Gen_Data(8,10)*Gen_Data(8,3));
        dt*Storage_Data(3,1)*Storage_Data(3,3)-Storage_Data(3,7);
        Storage_Data(3,7)];
  % Aeq Definition:
  %   Line 1:  Spot Market Coal
  %   Line 2:  Spot Market Nuclear
  %   Line 3:  Dispatchable Coal
  %   Line 4:  Dispatchable Hydro
  %   Line 5:  Dispatchable Gas
  %   Line 6:  Residential Load
  %   Line 7:  Commercial Load
  %   Line 8:  Industrail Load
  %   Line 9:  Load from PEV Slow Charge
  %   Line 10: Load from PEV Fast Charge
  %   Line 11: Energy from storage
  %   Line 12: Energy to storage
  Aeq =[(1-Line_Data(1,2))*dt*Gen_Data(4,1)*Gen_Data(4,3),...
        (1-Line_Data(1,2))*dt*Gen_Data(5,1)*Gen_Data(5,3),...
        dt*Gen_Data(6,1)*Gen_Data(6,3),...
        dt*Gen_Data(7,1)*Gen_Data(7,3),...
        dt*Gen_Data(8,1)*Gen_Data(8,3),...
        -Load_Data(1,7),...
        -Load_Data(2,7),...
        -Load_Data(3,7),...
        -Load_Data(5,7),...
        -Load_Data(6,7),...
        dt*Storage_Data(1,1)*Storage_Data(1,4),...
        -dt*Storage_Data(2,1)*Storage_Data(2,4)];

    beq = -sum(Gen_Data(1:3,9));

    lb = [0;0;0;0;0;0;0;0;0;0;0;0;0];
    ub = [1;1;1;1;1;1;1;1;1;1;1;1;1];

    [result, fval, flag] = intlinprog(f,intcon,A,b,Aeq,beq,lb,ub)

end
```

```
function result = Gen_Cost(Cost)

result = Cost(1)-Cost(2)+Cost(3);

end

function Update_Plot(IndVar,Daily_Data)

    %=========================================================================
    subplot(4,1,1)
    h1 = plot(IndVar,Daily_Data(1,:),IndVar,Daily_Data(2,:),...
              IndVar,Daily_Data(3,:),IndVar,Daily_Data(17,:));
    set(h1,'LineWidth',2)
    legend('R_S_o_l_a_r','R_W_i_n_d','R_H_y_d_r_o','Storage',...
           'location','northwest');
    ylabel('Energy (MWhr)')
    xlabel('Time Step (dt)')
    %=========================================================================
    subplot(4,1,2)
    h2 = plot(IndVar,Daily_Data(4,:),IndVar,Daily_Data(5,:),...
              IndVar,Daily_Data(6,:),IndVar,Daily_Data(7,:),...
              IndVar,Daily_Data(8,:))
    set(h2,'LineWidth',2)
    legend('SM_C_o_a_l','SM_N_u_c_l_e_a_r','D_C_o_a_l',...
           'D_H_y_d_r_o','D_L_P',...
           'location','northwest');
    ylabel('Energy (MWhr)')
    xlabel('Time Step (dt)')
    %=========================================================================
    subplot(4,1,3)
    h3 = plot(IndVar,Daily_Data(9,:),IndVar,Daily_Data(10,:),...
              IndVar,Daily_Data(11,:),IndVar,Daily_Data(12,:),...
              IndVar,Daily_Data(13,:))
    set(h3,'LineWidth',2);
    legend('L_R_e_s','L_C_o_m_m','L_I_n_d','L_E_V_S_C','L_H_V_D_C',...
           'location','northwest');
    ylabel('Energy (MWhr)')
    xlabel('Time Step (dt)')
    %=========================================================================
    subplot(4,1,4)
    h4 = plot(IndVar,Daily_Data(15,:),IndVar,Daily_Data(16,:))
    set(h4,'LineWidth',2);
    legend('G_t','L_t',...
           'location','northwest');
    ylabel('Energy (MWhr)')
    xlabel('Time Step (dt)')
```

```
        drawnow;
end
```